Magnetostructural Correlations in μ_2-1,1-N_3 Bridged, Dinuclear Copper(II) Complexes. 1. Ferromagnetic and Antiferromagnetic Coupling Associated with the Azide Bridge. X-ray Crystal Structures of $[Cu_2(DMPTD)(\mu_2\text{-}N_3)(\mu_2\text{-}Cl)Cl_2]\cdot CH_3CN$, $[Cu_2(DMPTD)(\mu_2\text{-}N_3)_2(N_3)_2]$, $[Cu_2(DIP)(\mu_2\text{-}N_3)(\mu_2\text{-}Cl)Cl_2]\cdot 0.5CH_3OH$, $[Cu_2(PAP46Me\text{-}H)(\mu_2\text{-}N_3)(N_3)_2]\cdot 0.33H_2O$, $[Cu_2(PAP)(\mu_2\text{-}N_3)Cl_3]\cdot CH_2Cl_2$, $[Cu_2(PAP)(\mu_2\text{-}N_3)(N_3)(NO_3)(CH_3OH)](NO_3)\cdot CH_3OH$, $[Cu_2(PPD3Me)(\mu_2\text{-}N_3)Cl_3(H_2O)_{1.5}]$, and $[Cu_2(PPD)(\mu_2\text{-}N_3)(NO_3)_3(H_2O)_{1.6}]$

Santokh S. Tandon, Laurence K. Thompson,* Mike E. Manuel, and John N. Bridson

Department of Chemistry, Memorial University of Newfoundland, St. John's, Newfoundland, Canada A1B 3X7

Received May 20, 1994[⊗]

A series of dinuclear, μ_2-1,1-azide bridged copper(II) complexes of seven tetradentate (N_4) diazine ligands has been prepared and characterized through spectroscopic, magnetochemical, and, in some cases, single-crystal X-ray diffraction studies: $[Cu_2(DMPTD)(\mu_2\text{-}N_3)(\mu_2\text{-}X)X_2]\cdot CH_3CN$ (X = Cl (**1**), Br (**2**)), $[Cu_2(DMPTD)(\mu_2\text{-}N_3)_2(N_3)_2]$ (**3**), $[Cu_2(DBITD)(\mu_2\text{-}N_3)_2Cl_2]\cdot H_2O$ (**4**), $[Cu_2(DIP)(\mu_2\text{-}N_3)(\mu_2\text{-}X)X_2]\cdot 0.5CH_3OH$ (X = Cl (**5**), X = Br (**6**)), $[Cu_2(PAP46Me\text{-}H)(\mu_2\text{-}N_3)(N_3)_2]\cdot 0.33H_2O$ (**7**), $[Cu_2(PAP)(\mu_2\text{-}N_3)Cl_3]\cdot CH_2Cl_2$ (**8**), $[Cu_2(PAP)(\mu_2\text{-}N_3)(N_3)(NO_3)(CH_3OH)](NO_3)\cdot CH_3OH$ (**9**), $[Cu_2(PPD3Me)(\mu_2\text{-}N_3)Cl_3(H_2O)_{1.5}]$ (**10**), $[Cu_2(PPD3Me)(\mu_2\text{-}N_3)Br_3]\cdot 0.5CH_3CN$ (**11**), $[Cu_2(PPD3Me)(\mu_2\text{-}N_3)(NO_3)_3]\cdot 0.5CH_3OH$ (**12**), and $[Cu_2(PPD)(\mu_2\text{-}N_3)(NO_3)_3(H_2O)_{1.6}]$ (**13**) (DMPTD = 2,5-bis((pyridylmethyl)thio) thiadiazole, DBITD = 2,5-bis(benzimidazolylmethyl)thio)thiadiazole, DIP = 3,6-bis(2′-imidazolyl-1′-methyl)thio)pyridazine, PAP46Me = 1,4-bis((4′,6′-dimethyl-2′-pyridyl)amino)phthalazine, PAP = 1,4-bis(2′-pyridylamino)phthalazine, PPD3Me = 3,6-bis(3′-methyl-1′-pyrazolyl)pyridazine), PPD = 3,6-bis(1′-pyrazolyl)pyridazine). Compound **1** crystallized in the monoclinic system, space group $P2_1/n$, with $a = 8.390(3)$ Å, $b = 24.857(2)$ Å, $c = 11.698(2)$ Å, $\beta = 93.38(2)°$, and $Z = 4$ ($R = 0.030$ and $R_w = 0.026$). Compound **3** crystallized in the triclinic system, space group $P\bar{1}$, with $a = 11.448(6)$ Å, $b = 11.541(5)$ Å, $c = 9.635(3)$ Å, $\alpha = 106.99(3)°$, $\beta = 90.99(4)°$, $\gamma = 71.41(3)°$, and $Z = 2$ ($R = 0.073$, $R_w = 0.060$). Compound **5** crystallized in the orthorhombic system, space group *Pnma*, with $a = 11.711(5)$ Å, $b = 21.713(8)$ Å, $c = 7.926(6)$ Å, and $Z = 4$ ($R = 0.113$, $R_w = 0.104$). Compound **7** crystallized in the monoclinic system, space group $P2_1$ with $a = 7.163(8)$ Å, $b = 16.074(7)$ Å, $c = 22.51(1)$ Å, $\beta = 93.4(1)°$, and $Z = 4$ ($R = 0.137$, $R_w = 0.135$). Compound **8** crystallized in the monoclinic system, space group $P2_1/c$ (No. 14), with $a = 13.382(2)$ Å, $b = 11.513(7)$ Å, $c = 16.424(2)$ Å, $\beta = 106.65(1)°$, and $Z = 4$ ($R = 0.029$, $R_w = 0.027$). Compound **9** crystallized in the triclinic system, space group $P\bar{1}$, with $a = 13.466(6)$ Å, $b = 14.833(5)$ Å, $c = 8.087(1)$ Å, $\alpha = 99.76(2)°$, $\beta = 107.35(2)°$, $\gamma = 63.16(3)°$, and $Z = 2$ ($R = 0.049$, $R_w = 0.038$). Compound **10** crystallized in the monoclinic system, space group $P2_1/n$ (No. 14), with $a = 10.909(2)$ Å, $b = 12.524(2)$ Å, $c = 14.744(2)$ Å, $\beta = 101.63(1)°$, and $Z = 4$ ($R = 0.046$, $R_w = 0.038$). Compound **13** crystallized in the monoclinic system, space group $P2_1/m$, with $a = 6.9617(9)$ Å, $b = 20.898(4)$ Å, $c = 7.568(1)$ Å, $\beta = 114.32(1)°$, and $Z = 2$ ($R = 0.062$, $R_w = 0.055$). In **1** and **2** the two square-pyramidal copper centers are bridged simultaneously by end-on μ_2-1,1-azido, halogen, and diazole groups, with one terminally bound halogen per square-pyramidal copper center. In **3** two essentially square-planar copper centers are bridged simultaneously by two equatorial μ_2-1,1-azides, with one terminal azide per metal. In **5** two distorted square-pyramidal copper centers are bridged equatorially by both the pyridazine (N_2) and μ_2-1,1-azide, and axially by a chlorine atom. In **7** each copper center has a distorted four-coordinate structure with one μ_2-1,1-azide and the phthalazine (N_2) bridging the two metals. In **8** one square-pyramidal copper center and one square-planar copper center are bridged equatorially by just two groups, the pyridazine (N_2) and μ_2-1,1-azide. In **9** a square-pyramidal and square-planar copper are bridged equatorially by a phthalazine (N_2) and μ_2-1,1-azide. In **10** two essentially square-planar copper centers are bridged equatorially by the pyridazine (N_2) and the μ_2-1,1-azide, while in **13** two square-pyramidal copper centers are bridged similarly. μ_2-1,1-azide bridge angles fall in the range 98.3−124.1°, which is unprecedented for azide-bridged dicopper(II) complexes. For **1**−**6** room temperature magnetic moments fall in the range 1.85−2.26 μ_B/Cu, while for **7**−**13** the moments fall below the spin only value (0.35−1.62 μ_B). Variable temperature magnetic studies (4−300 K) confirm the presence of moderate to strong net ferromagnetic interactions within each dinuclear unit for **1**−**6** ($2J = 60-170$ cm^{-1}), while for **7**−**13** net antiferromagnetic exchange prevails with $-2J$ falling in the range 40−1100 cm^{-1}, a most unusual feature of μ_2-1,1-azide bridged dicopper(II) complexes. A magnetostructural analysis of the complexes with equatorial diazine/μ_2-1,1-azide bridge combinations indicates that, contrary to the prevailing view, the μ_2-1,1-azide bridge can propagate antiferromagnetic coupling between two copper(II) centers if the bridge angle is large enough, and the critical angle for accidental orthogonality for the azide bridge is ≈108.5°.

Introduction

The magnetic properties of dinuclear coordination complexes, in particular those of copper, which involve spin exchange effects, have fascinated experimental and theoretical chemists for several decades. Of the very large number of simple dinuclear complexes reported, in which the metal ions are superexchange coupled, most exhibit antiferromagnetic behavior.[1-3] Magnetostructural correlations in dinuclear or polynuclear sys-

* Author to whom correspondence should be addressed.

⊗ Abstract published in *Advance ACS Abstracts,* October 15, 1994.

0020-1669/94/1333-5555$04.50/0

tems are not easily identified because the superexchange mechanism is affected by several structural parameters. The type and the magnitude of the magnetic exchange interaction depends on the bridge identity, the metal−metal separation, the bond angles subtended at the bridging atoms, the dihedral angles between the planes containing the metal ions, the metal−bridge ligand bond lengths, and the metal ion stereochemistries.[1-8] Considerable knowledge has been gained in understanding the magnetostructural relationships in symmetrical dibridged dinuclear metal complexes, in particular the dihydroxo-bridged copper(II) complexes studied by Hatfield et al.,[3] where a good linear relationship between exchange integral and hydroxide bridge angle was demonstrated. However only limited information is available about asymmetric dibridged and triply bridged dinuclear systems. In a series of asymmetric, antiferromagnetically coupled, dinuclear copper(II) complexes involving a diazine (phthalazine or pyridazine) and a hydroxide as equatorial magnetic bridges ($d_{x^2-y^2}$ ground state copper), a "linear" relationship between exchange integral and hydroxide bridge angle was demonstrated (Cu-OH-Cu 100−116°),[9] and the exchange process was considered to be dominated by the hydroxide.

In the last decade great efforts have been made to develop materials exhibiting ferromagnetic behavior and to determine what structural features, and which types of ligand could be used to specifically generate ferromagnetic complexes. Recently Hendrickson et al.[10,11] have reported magnetostructural properties of two triply bridged, ferromagnetically coupled, dinuclear copper(II) complexes involving dipyridyl ligands and combinations of carboxylate and hydroxide or water bridges, where the "noncomplimentary" nature of the metal bridging ligand overlap is cited as the major reason for net ferromagnetism. In a related study involving dibridged (hydroxide and carboxylate) *o*-phenanthroline complexes, Tokii et al. explain the strong net ferromagnetic coupling in terms of a small dihedral angle between the copper magnetic planes.[12] Castro et al.[13] have reported structural and magnetic properties of ferromagnetically coupled centrosymmetric ($2J = 17$ cm^{-1}) and asymmetric ($2J = 158$ cm^{-1}) copper(II) dimers present in the same unit cell and involving dihydroxy bridges, which complement the earlier studies by Hatfield et al.[3] Oshio et al.[14] reported structural and magnetic properties of ferromagnetically coupled oxalato-bridged, one-dimensional copper(II) complexes.

In dihydroxy-bridged dicopper(II) complexes the crossover from ferromagnetic to antiferromagnetic behavior occurs at about 97.5°,[3] and theoretical calculations have shown that for a less electronegative bridge like azide the critical angle for accidental orthogonality should occur above 103°.[2] However, in a separate study, the spin polarization effect is considered to possibly dominate the situation for all azide bridge angles.[15]

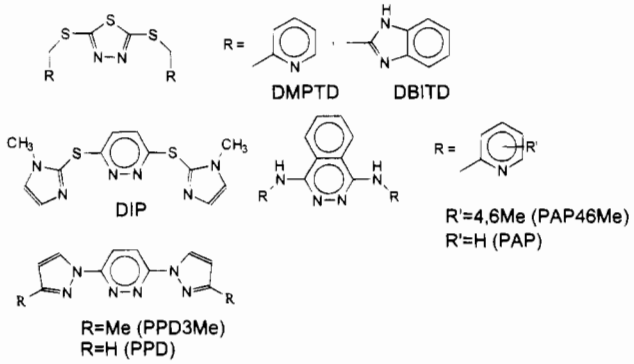

Figure 1. Tetradentate diazine ligands.

The dilemma stems, in part, from the paucity of μ_2-1,1-azide-bridged complexes that have been characterized both structurally and magnetically. In dinuclear copper(II) complexes involving either symmetric end-on (μ_2-1,1) azido bridges[15,16] or mixed bridges (μ_2-1,1-N_3 and μ_2-OH),[17] the ferromagnetic interactions between the copper centers have been attributed to the spin polarization effects associated with the μ_2-1,1-azido groups. μ_2-1,1-Azide bridges have been shown to propagate ferromagnetic coupling in dinickel(II) complexes,[18] and the concept of spin polarization has recently been supported by Ribas et al.,[19] in order to explain the ferromagnetic interaction in dinuclear and tetranuclear nickel(II) complexes involving end-on azido bridges.

In an earlier communication,[20] we reported the X-ray crystal structure and magnetic properties of a dinuclear, ferromagnetically coupled copper(II) complex, $[Cu_2(DMPTD)(\mu_2\text{-}Br)(\mu_2\text{-}N_3)Br_2]\cdot CH_3CN$ (2), of the tetradentate (N_4), dinucleating ligand 2,5-bis((pyridylmethyl)thio)thiadiazole (DMPTD). In this paper we report the synthesis, structural characterization, and variable temperature magnetic studies on a series of μ_2-1,1-azide-bridged dinuclear copper(II) complexes of seven tetradentate diazine ligands (Figure 1), some of which exhibit moderate to strong ferromagnetic exchange ($2J > 60$ cm^{-1}), while others exhibit moderate to strong net antiferromagnetic exchange ($-2J = 40-1100$ cm^{-1}). For the first time the μ_2-1,1-azide bridge has been shown to propagate antiferromagnetic exchange at large bridge angles ($> \approx 108°$), indicating that, as in the case of the μ_2-OH bridge, magnetic properties associated with the azide bridge are bridge angle dependent, and the change from ferromagnetic to antiferromagnetic behavior occurs at ≈108.5°. Also an analysis of the ν_{as} azide infrared absorptions reveals that in general μ_2-1,1-azide bridges are associated with bands at $> \approx 2055$ cm^{-1}.

Experimental Section

Synthesis of Ligands: (a) 2,5-Bis((pyridylmethyl)thio)thiadiazole (DMPTD). Sodium metal (3.70 g, 160 mmol) was dissolved in dry (O_2 free) methanol (200 mL) by stirring at room temperature for 30 min (N_2 atmosphere) and solid 2,5-dimercapto-1,3,4-thiadiazole (6.00 g, 40 mmol) was added. The resulting light brown solution was stirred at −5 to 0 °C for 1 h and 2-picolylchloride dissolved in dry methanol

(1) Kahn, O. *Comments Inorg. Chem.* **1984**, *3*, 105.
(2) Kahn, O. *Inorg. Chim. Acta* **1982**, *62*, 3.
(3) Crawford, V. H.; Richardson, H. W.; Wasson, J. R.; Hodgson, D. J.; Hatfield, W. E. *Inorg. Chem.* **1976**, *15*, 2107.
(4) Hodgson, D. J. *Prog. Inorg. Chem.* **1975**, *19*, 173.
(5) Doedens, R. J. *Prog. Inorg. Chem.* **1976**, *21*, 209.
(6) Melnik, M. *Coord. Chem. Rev.* **1982**, *42*, 259.
(7) Kahn, O. Angew. *Chem. Int., Ed. Engl.* **1985**, *24*, 834.
(8) Kato, M.; Muto, Y. *Coord. Chem. Rev.* **1988**, *92*, 45.
(9) Thompson, L. K.; Lee, F. L.; Gabe, E. J. *Inorg. Chem.* **1988**, *27*, 39.
(10) Christou, G.; Perlepes, S. P.; Folting, K.; Huffman, J. C.; Webb, R. J.; Hendrickson, D. N. *J. Chem. Soc., Chem. Commun.* **1990**, 746.
(11) Christou, G.; Perlepes, S. P.; Libby, E.; Folting, K.; Huffman, J. C.; Webb, R. J.; Hendrickson, D. N. J. *Inorg. Chem.* **1990**, *29*, 3657.
(12) Tokii, T.; Hamamura, N.; Nakashima, M.; Muto, Y. *Bull. Chem. Soc. Jpn.* **1992**, *65*, 1214.
(13) Castro, I.; Faus, J.; Julve, M.; Bois, C.; Real, J. A.; Lloret, F. *J. Chem. Soc., Dalton Trans.* **1992**, 47.
(14) Oshio, H.; Nagashima, U. *Inorg. Chem.* **1992**, *31*, 3295.
(15) Sikorav, S.; Bkouche-Waksman, I.; Kahn, O. *Inorg. Chem.* **1984**, *23*, 490.
(16) Comarmond, J.; Plumeré, P.; Lehn, J.-M.; Agnus, Y.; Louis, R.; Weiss, R.; Kahn, O.; Morgenstern-Badarau, I. *J. Am. Chem. Soc.* **1982**, *104*, 6330.
(17) Kahn, O.; Sikorav, S.; Gouteron, J.; Jeannin, S.; Jeannin, Y. *Inorg. Chem.* **1983**, *22*, 2877.
(18) Cortes, R.; Ruiz de Larramendi, J. I.; Lezama, L.; Rojo, T.; Urtiaga, K.; Arriortua, M. I. *J. Chem. Soc., Dalton Trans.* **1992**, 2723.
(19) Ribas, J.; Monfort, M.; Costa, R.; Solans, X. *Inorg. Chem.* **1993**, *32*, 695.
(20) Tandon, S. S.; Thompson, L. K.; Bridson, J. N. *J. Chem. Soc., Chem. Commun.* **1993**, 804.

(O_2 free) (100 mL) added dropwise over a period of 1.5 h, keeping the temperature at ca. 0 °C. After complete addition, the resulting mixture was stirred at 0 °C for 1 h, then at 60−70 °C for 4 h and finally at room temperature for 16 h. A white solid (NaCl) separated, which was filtered off, and the filtrate was concentrated under reduced pressure at 30 °C to give an oily mass which solidified on cooling to produce a white crystalline compound. It was characterized through mass and NMR spectra. Yield: 68%. Mass spectrum (*m/z*) (major mass peaks; relative intensity): 332 (0.5) (M), 240 (7), 208 (85), 150 (27), 136 (12), 124 (24), 92 (100). ^{1}H NMR ($CDCl_3$) (δ, ppm (relative intensity)): 5.79 (singlet, 4H, CH_2), 7.22 (triplet, 2H, Py), 7.46 (doublet, 2H, Py), 7.65 (triplet, 2H, Py), 8.57 (doublet, 2H, Py).

2,5-Bis((benzimidazolylmethyl)thio)thiadiazole (DBITD). Solid 2,5-dimercapto-1,3,4-thiadiazole (5.0 g, 33 mmol) was added to a solution of sodium methoxide prepared by the addition of sodium metal (1.53 g, 66 mmol) to dry methanol (150 mL) (under N_2 atmosphere) at 0 °C and the resulting mixture was stirred at this temperature for 1 h. A solution of 2-chloromethyl benzimidazole (11.1 g, 0.067 mol) in hot methanol (100 mL) was added dropwise over a period of 1.5 h, maintaining the temperature at ca. 0 °C. The resulting mixture was stirred at 0 °C for 1 h, 60−70 °C for 4 h and then at room temperature for 16 h. A pale yellow solid separated, which was filtered off, washed with water (3 × 20 mL) to remove NaCl, ethanol (3 × 5 mL) and finally with ether (3 × 20 mL) and dried under vacuum. Mp: 228−230 °C; yield 84%. Mass spectrum (*m/z*) (major mass peaks; relative intensity) 378 (6.4) (M − H_2S), 259 (20), 208 (12), 179 (16), 162 (30), 151 (47), 132 (100), 118 (34), 92 (29). ^{1}H NMR (DMSO-d_6) (δ, ppm (relative intensity)): 3.40 (singlet, 2H, NH), 4.74 (singlet, 4H, CH_2), 7.15 (doublet, 4H, Ph), 7.50 (triplet, 4H, Ph).

3,6-Bis(3′-methyl-1′-pyrazolyl)pyridazine (PPD3Me). 3-Methylpyrazole (5.0 g, 0.061 mol) was dissolved in dry THF (150 mL) under nitrogen. Potassium metal (2.5 g, 0.064 mol), cut into small pieces, was added and the mixture stirred under nitrogen until all the potassium dissolved. 3,6-Dichloropyridazine (4.0 g, 0.027 mol) was added to the clear solution, and the mixture was refluxed for several hours. The red-brown solution was allowed to cool and stand overnight. A dirty white precipitate formed, which was filtered off, washed with water to remove KCl, and dried under vacuum. Mp: 254−256 °C; yield 45% (recrystallization from $CHCl_3$ gave white crystals, mp 255−256 °C). Mass spectrum (*m/z*) (major mass peaks; relative intensity): 240 (100), 170 (10), 119 (12), 94 (7), 78 (8), 67 (7), 52 (13). ^{1}H NMR ($CDCl_3$) (δ, ppm (relative intensity)); 2.39 (3) (CH_3), 6.34 (1) (pyrazole H_4), 8.26 (1) (pyrazole H_5), 8.61 (1) (pyridazine).

Synthesis of Complexes. (a) $[Cu_2(DMPTD)(\mu_2\text{-}N_3)(\mu_2\text{-}Cl)Cl_2]\cdot CH_3CN$ (1), $[Cu_2(DMPTD)(\mu_2\text{-}N_3)(\mu_2\text{-}Br)Br_2]\cdot CH_3CN$ (2), $[Cu_2(DMPTD)(\mu_2\text{-}N_3)_2(N_3)_2]\cdot CH_3OH$ (3). 2,5-Bis((pyridylmethyl)thio)-thiadiazole (DMPTD) (0.10 g, 0.30 mmol), dissolved in a 1:1 mixture of acetonitrile/methanol (40 mL), was added to a solution of $CuCl_2\cdot 2H_2O$ (0.17g, 1.00 mmol) in methanol (20 mL). The resulting green solution was stirred at room temperature for 5−10 min and a solution of NaN_3 (0.065 g, 1.0 mmol) in hot methanol (20 mL) added dropwise. The resulting dark green mixture was filtered and the filtrate produced crystals suitable for X-ray analysis upon standing at room temperature for a few days. Yield: 45%. Anal. Calcd for $[Cu_2(C_{14}H_{12}N_4S_3)(\mu_2\text{-}N_3)(\mu_2\text{-}Cl)Cl_2]\cdot CH_3CN$ (**1**): C, 29.61; H, 1.86; N, 17.26; Cu, 19.58. Found: C, 29.24; H, 2.26; N, 17.93; Cu, 19.15. Compound **2** was prepared similarly.[20]

$Cu(NO_3)_2\cdot 3H_2O$ (0.20 g, 0.80 mmol) was dissolved in a 1:1 mixture of DMF/acetonitrile (20 mL). DMPTD (0.10 g, 0.30 mmol) was added and the mixture stirred at room temperature for 5 min. A solution of NaN_3 (0.040 g, 0.62 mmol) dissolved in hot methanol (10 mL) was added. The resulting green solution produced a small quantity of green crystals (**3**) on standing overnight. These were used in a preliminary X-ray analysis. A second crop of product (yield 20 mg, 10%) was subjected to microanalysis and shown to contain one methanol molecule. Anal. Calcd for $[Cu_2(C_{14}H_{12}N_4S_3)(\mu_2\text{-}N_3)_2(N_3)_2]\cdot CH_3OH$ (**3**): C, 27.31; H, 2.44; N, 33.97; Cu, 19.27. Found: C, 27.16; H, 1.94; N, 33.44; Cu, 19.61.

The same complex was produced by reaction of $Cu(ClO_4)_2\cdot 6H_2O$ (0.81 mmol), DMPTD (0.3 mmol), and NaN_3 (1.2 mmol) in a 1:1:1 methanol/acetonitrile/DMF mixture (30 mL) as green crystals (yield 64%). An X-ray structure revealed the same structural unit. The structural data reported in this paper are for the complex prepared from $Cu(ClO_4)_2$, which was shown to be unsolvated.

(b) $[Cu_2(DBITD)(\mu_2\text{-}N_3)_2Cl_2]\cdot H_2O$ (4). 2,5-Bis((benzimidazolylmethyl)thio)thiadiazole (DBITD) (0.10 g, 0.25 mmol) was dissolved in a 1:1 mixture of methanol/ dichloromethane (40 mL) by stirring at room temperature for 10 min and was added to a solution of $CuCl_2\cdot 2H_2O$ (0.18 g, 1.0 mmol) in methanol (20 mL). The resulting green solution was stirred at room temperature for 10 min and a solution of sodium azide (0.030 g, 0.5 mmol) in hot methanol (20 mL) added dropwise. An olive green solution formed, which was filtered, and the filtrate allowed to stand at room temperature overnight. Green crystals of 4 formed, which were washed with methanol (3 × 5 mL) and dried under vacuum. Yield: 44%. Anal. Calcd for $[Cu_2(C_{18}H_{14}N_6S_3)(\mu_2\text{-}N_3)_2\text{-}Cl_2]\cdot H_2O$ (**4**): C, 30.42; H,2.27; N, 23.65; Cu, 17.88. Found: C, 30.58; H, 2.09; N, 22.96; Cu, 18.25.

(c) $[Cu_2(DIP)(\mu_2\text{-}N_3)(\mu_2\text{-}X)X_2]\cdot 0.5CH_3OH$ (X = Cl (5); X = Br (6)). $CuCl_2\cdot 2H_2O$ (0.30 g, 1.8 mmol) was dissolved in a 1:1 mixture of methanol/acetonitrile (30 mL) and a solution of DIP[21] (0.10 g, 0.30 mmol) in the same solvent mixture (10 mL) added, followed by a solution of NaN_3 (0.10 g, 1.5 mmol) dissolved in hot methanol (10 mL). The reaction mixture was stirred at room temperature for 10 min and allowed to stand overnight. Olive green needles formed, which were filtered off, washed with methanol (3 × 5 mL), and dried under vacuum. Yield: 45%. Anal. Calcd for $[Cu_2(C_{12}H_{12}N_4S_2)(N_3)Cl_3]\cdot 0.5\text{-}CH_3OH$ (**5**): C, 25.20; H, 2.35; N, 21.16. Found: C, 25.23; H, 2.15; N, 20.85.

DIP (0.10 g, 0.30 mmol) was dissolved in methanol (25 mL) and a solution of $CuBr_2$ (0.25 g, 1.1 mmol) in a 1:1:1 mixture of DMF/ methanol/acetonitrile added. A solution of NaN_3 (0.030 g, 0.50 mmol) in hot methanol (15 mL) was added to the bright green solution. An olive green solution formed, which was filtered, and the filtrate allowed to stand overnight at room temperature. An olive green crystalline solid formed (**6**), which was filtered off, washed with methanol (3 × 5 mL), and dried under vacuum. Yield: 50%. Anal. Calcd for $[Cu_2\text{-}(C_{12}H_{12}N_4S_2)(N_3)Br_3]\cdot 0.5CH_3OH$ (**8**): C, 20.59; H, 1.92; N, 17.29; Cu, 17.43. Found: C, 20.74; H, 1.80; N, 17.42; Cu, 17.70.

(d) $[Cu_2(PAP46Me\text{-}H)(\mu_2\text{-}N_3)(N_3)_2]\cdot 0.33H_2O$ (7). $[Cu_2(PAP46Me)\text{-}(OH)Cl_3]\cdot EtOH$[22] (0.20 g, 0.33 mmol) was dissolved in 50% CH_3CN/ H_2O (30 mL), and a solution of NaN_3 (0.100 g, 1.5 mmol) dissolved in water (30 mL) was added with stirring. A khaki precipitate formed, which was filtered off, washed with water and acetonitrile, and air-dried. Recrystallization was effected by slow diffusion of diethyl ether into a DMF solution of the complex, forming khaki crystals of **7**. Anal. Calcd for $[Cu_2(C_{22}H_{21}N_6)(N_3)_3]\cdot 0.33H_2O$: C, 42.04; H, 3.45; N, 33.42. Found: C, 42.06; H, 3.50; N, 33.25.

(e) $[Cu_2(PAP)(\mu_2\text{-}N_3)Cl_3]\cdot CH_2Cl_2$ (8), $[Cu_2(PAP)(\mu_2\text{-}N_3)(N_3)(NO_3)\text{-}(CH_3OH)](NO_3)\cdot CH_3OH$ (9), $[Cu_2(PPD3Me)(\mu_2\text{-}N_3)Cl_3(H_2O)_{1.5}]$ (10), $[Cu_2(PPD3Me)(\mu_2\text{-}N_3)Br_3]\cdot 0.5CH_3CN$ (11), $[Cu_2(PPD3Me)(\mu_2\text{-}N_3)\text{-}(NO_3)_3]\cdot 0.5CH_3OH$ (12), $[Cu_2(PPD)(\mu_2\text{-}N_3)(H_2O)_{1.6}]$ (13). $CuCl_2\cdot 2H_2O$ (0.12 g, 0.7 mmol) was dissolved in hot MeOH (20 mL) and added to a solution of PAP[23] (0.100 g, 0.32 mmol) dissolved in hot CH_2Cl_2 (20 mL). A solution of NaN_3 (0.045 g, 0.7 mmol) dissolved in hot MeOH (10 mL) was added immediately. A small quantity of green crystals formed, which were filtered off, and the filtrate allowed to stand at room temperature for 2 days. Dark green crystals formed, which were filtered off, washed with MeOH (20 mL), and dried under vacuum. Yield 30%. Anal. Calcd for $[Cu_2(C_{18}H_{14}N_6)(N_3)Cl_3]\cdot CH_2Cl_2$ (**8**): C, 33.82; H, 2.39; N, 18.68. Found: C, 34.36; H, 2.57; N, 18.96. **9** was prepared similarly. Yield 40%. Anal. Calcd for $[Cu_2(C_{18}H_{14}N_6)\text{-}(N_3)_2(NO_3)_2\cdot CH_3OH]\cdot CH_3OH$. H_2O (**9**): C, 32.84; H, 3.31; N, 26.81. Found: C, 32.76; H, 2.97; N, 26.58.

A solution of $CuCl_2\cdot 2H_2O$ (0.10 g, 0.6 mmol) in methanol (15 mL) was added to a suspension of PPD3Me (0.050 g, 0.21 mmol) in acetonitrile (15 mL). Water (1 mL) was added with the formation of a dark green solution, which was heated on a steam bath for several

(21) Woon, T. C.; McDonald, R.; Mandal, S. K.; Thompson, L. K.; Connors, S. P.; Addison, A. W. *J. Chem. Soc., Dalton Trans.* **1986**, 2381.
(22) Bullock, G.; Hartstock, F. W.; Thompson, L. K. *Can. J. Chem.* **1983**, *61*, 57.
(23) Thompson, L. K.; Chacko, V. T.; Elvidge, J. A.; Lever, A. B. P.; Parish, R. V. *Can. J. Chem.* **1969**, *47*, 4141.

minutes. A solution of NaN_3 (0.020 g, 0.31 mmol) in water (2 mL) was then added dropwise and the mixture stirred. A khaki green solution formed, which was allowed to evaporate slowly over a few days with the formation of green crystals of **10**. Some crystals were separated for X-ray analysis, and the main product was filtered off, washed with H_2O/MeOH (2:1; 2 × 1 mL), and dried under vacuum. Yield: 35%. Anal. Calcd for $[Cu_2(C_{12}H_{12}N_6)(N_3)Cl_3(H_2O)\cdot 0.5CH_3OH$ (**10**): C, 27.31; H, 2.91; N, 22.93. Found: C, 27.16; H, 2.77; N, 23.04. **11** and **12** were prepared similarly using $CuBr_2$ and $Cu(NO_3)_2\cdot 3H_2O$ respectively. Anal. Calcd for $[Cu_2(C_{12}H_{12}N_6)(N_3)Br_3]\cdot 0.5CH_3CN$ (**11**): C, 23.31; H, 2.03; N, 19.87. Found: C, 23.23; H, 2.17; N, 19.56. Anal. Calcd for $[Cu_2(C_{12}H_{12}N_6)(NO_3)_3]\cdot 0.5CH_3OH$ (**12**): C, 24.56; H, 2.29; N, 27.49. Found: C, 24.59; H, 2.52; N, 27.39. **13** was prepared similarly using PPD[24] and $Cu(NO_3)_2\cdot 3H_2O$. Anal. Calcd for $[Cu_2(C_{10}H_8N_6)(N_3)(NO_3)_3]\cdot CH_3OH$ (**13**): C, 22.05; H, 2.00; N, 28.05. Found: C, 22.36; H, 2.07; N, 28.49. The crystals chosen for X-ray study were prepared separately and shown not to contain methanol.

Physical Measurements. NMR spectra were recorded with a GE 300 MHz spectrometer ($SiMe_4$ internal standard), and mass spectra were obtained with a VG Micromass 7070 HS spectrometer with a direct insertion probe. Electronic spectra were recorded as mulls and in DMF solutions using a Cary 5E spectrometer. Infrared spectra were recorded as Nujol mulls using a Mattson Polaris FT-IR instrument. Microanalyses were carried out by Canadian Microanalytical Service, Delta, Canada. Room temperature magnetic susceptibilities were measured by the Faraday method using a Cahn 7600 Faraday magnetic balance and variable temperature magnetic data (4−300 K) were obtained using an Oxford Instruments superconducting Faraday Susceptometer with a Sartorius 4432 microbalance. A main solenoid field of 1.5 T and a gradient field of 10 T m^{-1} were employed.

Safety Note. *Caution!* Azide compounds are potentially explosive and should be treated with care and in small quantities. In particular, copper(II) azide is explosive, and in those reactions where an excess of copper(II) salt is used, followed by addition of azide, an excess of azide should be avoided. A small explosion resulted when a small quantity of a solid azide complex, which was synthesized in this way, was handled. This was attributed to copper azide impurity. Most of the complexes reported here were synthesized by adding limited amounts of sodium azide and did not produce explosive material.

Crystallographic Data Collection and Refinement of the Structures. $[Cu_2(DMPTD)(\mu_2\text{-}N_3)(\mu_2\text{-}Cl)Cl_2]\cdot CH_3CN$ (1). The crystals of **1** are brown. The diffraction intensities of an approximately 0.35 × 0.25 × 0.15 mm crystal were collected with graphite-monochromatized Mo Kα radiation using a Rigaku AFC6S diffractometer at 26 ± 1 °C and the $\omega-2\theta$ scan technique to a $2\theta_{max}$ value of 50.0°. A total of 4704 reflections were measured, of which 4394 (R_{int} = 0.025) were unique and 3201 were considered significant with $I_{net} > 2.0\sigma(I_{net})$. An empirical absorption correction was applied, after a full isotropic refinement, using the program DIFABS,[25] which resulted in transmission factors ranging from 0.83 to 1.00. The data were corrected for Lorentz and polarization effects. The cell parameters were obtained from the least-squares refinement of the setting angles of 23 carefully centered reflections with 2θ in the range 20.58−29.02°.

The structure was solved by direct methods.[26,27] The non-hydrogen atoms were refined anisotropically. The final cycle of full-matrix least-squares refinement was based on 3201 observed reflections ($I > 2.00\sigma(I)$) and 290 variable parameters and converged with unweighted and weighted agreement factors of $R = \sum||F_o| - |F_c||/\sum|F_o| = 0.030$ and $R_w = [(\sum w(|F_o| - |F_c|)^2/\sum wF_o2)]^{1/2} = 0.026$. The maximum and minimum peaks on the final difference Fourier map correspond to +0.30 and −0.29 electron/Å^3 respectively. Neutral-atom scattering factors[28] and anomalous-dispersion terms[29,30] were taken from the usual sources. All calculations were performed with the TEXSAN[31] crystallographic software package using a VAX 3100 work station. A summary of the crystal and other data is given in Table 1, and atomic coordinates are given in Table 2. Hydrogen atom atomic coordinates (Table S1), anisotropic thermal parameters (Table S2), a full listing of bond distances and angles (Table S3), and least-squares planes data (Table S4) are included as supplementary material.

$[Cu_2(DMPTD)(\mu_2\text{-}N_3)_2(N_3)_2]$ (3). The diffraction intensities of a green regular polyhedral crystal of approximate dimensions 0.30 × 0.15 × 0.15 mm were collected on a Rigaku AFC6S diffractometer, with graphite-monochromatized Mo Kα radiation. The data were collected at a temperature of 26 ± 1 °C using the $\omega-2\theta$ scan technique to a maximum 2θ value of 50.1°. Cell constants were obtained by the least squares refinement of the setting angles of 22 carefully centered reflections with 2θ in the range 25.93−30.22°. A total of 4300 reflections were measured, of which 4075 were unique (R_{int} = 0.041), and 2024 were considered significant with $I_{net} > 2.00\sigma(I_{net})$. The intensities of three representative reflections which were measured after every 150 reflections declined by −11.00%. Some crystal decomposition occurs in the X-ray beam. A linear correction factor was applied to the data to account for this phenomenon. An empirical absorption correction, based on azimuthal scans of several reflections, was applied which resulted in transmission factors ranging from 0.41 to 1.32. The data were corrected for Lorentz and polarization effects.

The structure was solved by direct methods.[26,27] One terminal azide group in the structure appears to be disordered, and has been modeled as a "wagging" azide. The non-hydrogen atoms were refined anisotropically, and the hydrogen atoms introduced in calculated positions with isotropic thermal parameters set 20% greater than their bonding partners. They were included, but not refined in the final rounds of least squares. The final cycle of full-matrix least-squares refinement was based on 2024 observed reflections ($I > 2.00\sigma(I)$) and 246 variable parameters and converged with unweighted and weighted agreement factors of $R = \sum||F_o| - |F_c||/\sum|F_o| = 0.070$ and $R_w = [(\sum w(|F_o| - |F_c|)^2/\sum wF_o2)]^{1/2} = 0.057$. The maximum and minimum peaks on the final difference Fourier map correspond to +0.65 and −0.77 electron/Å^3, respectively. Neutral-atom scattering factors[28] and anomalous-dispersion terms[29,30] were taken from the usual sources. All calculations were performed with the TEXSAN[31] crystallographic software package using a VAX 3100 work station. A summary of the crystal and other data is given in Table 1, and atomic coordinates are given in Table 3. Hydrogen atom atomic coordinates (Table S5), anisotropic thermal parameters (Table S6), a full listing of bond distances and angles (Table S7), and least-squares planes data (Table S8) are included as supplementary material.

A structural determination on the same complex obtained from copper nitrate showed similar crystal instability and a disordered terminal azide, but because of a poorer data to parameter ratio, the result for compound **3** prepared from $Cu(ClO_4)_2$ is discussed.

$[Cu_2(DIP)(\mu_2\text{-}N_3)(\mu_2\text{-}Cl)Cl_2]\cdot 0.5CH_3OH$ (5). Diffraction data were collected for a small, poorly diffracting, green platelike crystal of approximate dimensions 0.40 × 0.15 × 0.07 mm. The geometry of the unit cell and symmetry in the diffraction pattern of the crystal supported an orthorhombic space group, but the weak data set prevented unambiguous space group assignment. The structure was solved in various monoclinic space groups to identify, beyond all doubt, the symmetry elements present, and then the asymmetric unit was reoriented and positioned in the correct orthorhombic cell. Subsequent refinement gave poor R values, attributable to the poor data set. Crystal and other data are given in Table 1, but the solution must be considered preliminary at this stage.

$[Cu_2(PAP46Me\text{-}H)(\mu_2\text{-}N_3)(N_3)_2]$ (7). Diffraction data were collected for a black, irregular crystal of approximate dimensions 0.30 × 0.30 × 0.080 mm. The odd shape of the crystal suggested that it was a multiple crystal, and when a portion cut from a cluster was mounted, it turned out to be nonsingle. However a reasonable data set was

(24) Thompson, L. K.; Woon, T. C.; Murphy, D. B.; Gabe, E. J.; Lee, F. L.; Le Page, Y. *Inorg. Chem.* **1985**, *24*, 4719.
(25) Walker, N.; Stuart, D. *Acta Crystallogr.* **1983**, *A39*, 158.
(26) Gilmore, C. J. *J. Appl. Crystallogr.* **1984**, *17*, 42.
(27) Beurskens, P. T. DIRDIF: Technical Report 1984/1, Crystallography Laboratory: Toernooiveld, 6525 Ed Nijmegen, Netherlands, 1984.
(28) Cromer, D. T.; Waber, J. T. International Tables for X-ray Crystallography; The Kynoch Press: Birmingham, U.K. 1974; Vol. IV, Table 2.2A.
(29) Ibers, J. A.; Hamilton, W. C. *Acta Crystallogr.* **1974**, *17*, 781.
(30) Cromer, D. T. *International Tables for X-ray Crystallography*; The Kynoch Press: Birmingham, U.K. 1974; Vol. IV, Table 2.3.1.
(31) Texsan-Texray Structure Analysis Package. Molecular Structure Corporation, 1985.

Table 1. Summary of Crystallographic Data for $[Cu_2(DMPTD)(\mu_2\text{-}N_3)(\mu_2\text{-}Cl)Cl_2]\cdot CH_3CN$ (**1**), $[Cu_2(DMPTD)(\mu_2\text{-}N_3)_2(N_3)_2]$ (**3**), $[Cu_2(DIP)(\mu_2\text{-}N_3)Cl_3]$ (**5**), $[Cu_2(PAP46Me\text{-}H)(\mu_2\text{-}N_3)(N_3)_2]$ (**7**), $[Cu_2(PAP)(\mu_2\text{-}N_3)Cl_3]\cdot CH_2Cl_2$ (**8**), $[Cu_2(PAP)(\mu_2\text{-}N_3)(N_3)(NO_3)(CH_3OH)](NO_3)\cdot CH_3OH$ (**9**), $[Cu_2(PPD3Me)(\mu_2\text{-}N_3)Cl_3(H_2O)_{1.5}]$ (**10**), and $[Cu_2(PPD)(\mu_2\text{-}N_3)(NO_3)_3(H_2O)_{1.6}]$ (**13**)

	1	**3**	**5**	**7**	**8**	**9**	**10**	**13**
empirical formula	$C_{16}H_{15}N_8S_3Cl_3Cu_2$	$C_{14}H_{12}N_{16}S_3Cu_2$	$C_{12}H_{16}N_9S_2Cu_2Cl_3$	$C_{24}H_{25}O_{0.5}N_{15}Cu_2$	$C_{19}H_{16}N_9Cu_2Cl_5$	$C_{20}H_{22}N_{14}Cu_2O_8$	$C_{12}H_{15}N_9Cu_2Cl_3O_{1.5}$	$C_{10}H_{11.1}N_{12}O_{10.6}Cu_2$
fw	648.98	627.63	583.89	630.64	674.75	713.57	542.76	596.16
space group	$P2_1/n$	$P\bar{1}$	*Pnma* (No. 62)	$P2_1$ (No. 4)	$P2_1/c$ (No. 14)	$P\bar{1}$	$P2_1/n$ (No. 14)	$P2_1/m$ (No. 11)
a (Å)	8.390(3)	11.448(6)	11.711(5)	7.163(8)	13.382(2)	13.466(6)	10.909(2)	6.9617(9)
b (Å)	24.857(2)	11.541(5)	21.713(8)	16.074(7)	11.513(7)	14.833(5)	12.524(2)	20.898(4)
c (Å)	11.698(2)	9.635(3)	7.926(6)	22.51(1)	16.424(2)	8.087(1)	14.744(2)	7.568(1)
α (deg)		106.99(3)				99.76(2)		
β (deg)	93.38(2)	90.99(4)		93.4(1)	106.65(1)	107.35(2)	101.63(1)	114.32(1)
γ (deg)		71.41(3)				63.16(3)		
V (Å^3)	2435(1)	1149.8(9)	2016(2)	2587(4)	2424(1)	1375(1)	1973.1(6)	1003.4(1)
ϱ_{calcd} (g cm^{-3})	1.770	1.813	1.924	1.619	1.849	1.724	1.827	1.973
Z	4	2	4	4	4	2	4	2
μ (cm^{-1})	23.54	21.57	27.38	16.91	23.45	16.21	25.98	22.06
λ (Å)	0.710 69	0.710 69	0.710 69	0.710 69	0.710 69	0.710 69	0.710 69	0.710 69
T (°C)	26	26	26	25	26	26	26	26
R	0.030	0.073	0.113	0.137	0.029	0.049	0.046	0.062
R_w	0.026	0.060	0.104	0.135	0.027	0.038	0.038	0.055

[a] $R = \sum||F_o| - |F_c||/\sum|F_o|$, $R_w = [(\sum w(|F_o| - |F_c|)^2/\sum wF_o^2)]^{1/2}$.

Table 2. Final Atomic Positional Parameters and B(eq) Values for $[Cu_2(DMPTD)(\mu_2\text{-}N_3)(\mu_2\text{-}Cl)Cl_2]\cdot CH_3CN$ (**1**)

atom	x	y	z	B(eq)[a] (Å^2)
Cu(1)	0.83733(6)	0.08315(2)	0.23783(4)	3.43(2)
Cu(2)	0.88548(6)	0.17170(2)	0.42589(4)	3.41(2)
Cl(1)	0.6699(1)	0.10377(4)	0.40420(8)	3.78(4)
Cl(2)	0.7818(1)	0.09934(4)	0.05016(8)	4.69(5)
Cl(3)	0.8861(1)	0.26199(4)	0.40508(8)	4.55(5)
S(1)	1.1213(1)	−0.03879(4)	0.30325(9)	3.99(5)
S(2)	1.2727(1)	0.02982(4)	0.48785(9)	4.09(5)
S(3)	1.2854(1)	0.13301(5)	0.6147(1)	4.82(6)
N(1)	0.7582(4)	0.0082(1)	0.2108(2)	3.3(1)
N(2)	1.0282(3)	0.0621(1)	0.3668(2)	2.9(1)
N(3)	1.0678(3)	0.1039(1)	0.4428(2)	2.9(1)
N(4)	0.8749(3)	0.1766(1)	0.5947(2)	2.9(1)
N(5)	0.9114(4)	0.1573(1)	0.2645(2)	4.3(2)
N(6)	0.9484(4)	0.1887(1)	0.1924(3)	3.7(2)
N(7)	0.9820(5)	0.2182(2)	0.1241(3)	6.2(2)
N(8)	0.7767(5)	0.4124(2)	0.6868(3)	6.3(2)
C(1)	0.6000(5)	−0.0000(2)	0.2084(3)	4.0(2)
C(2)	0.5279(5)	−0.0433(2)	0.1518(3)	4.6(2)
C(3)	0.6198(5)	−0.0791(2)	0.0956(3)	4.6(2)
C(4)	0.7822(5)	−0.0719(2)	0.1009(3)	3.9(2)
C(5)	0.8488(4)	−0.0281(1)	0.1586(3)	3.1(2)
C(6)	1.0252(5)	−0.0190(1)	0.1656(3)	3.8(2)
C(7)	1.1246(4)	0.0212(1)	0.3806(3)	3.0(2)
C(8)	1.1922(4)	0.0927(1)	0.5090(3)	3.3(2)
C(9)	1.1600(5)	0.1928(2)	0.6105(3)	4.3(2)
C(10)	1.0043(5)	0.1857(1)	0.6639(3)	3.3(2)
C(11)	0.9952(5)	0.1896(2)	0.7819(3)	4.2(2)
C(12)	0.8492(6)	0.1852(2)	0.8279(3)	4.9(2)
C(13)	0.7153(5)	0.1773(2)	0.7571(4)	4.4(2)
C(14)	0.7324(5)	0.1728(1)	0.6409(3)	3.6(2)
C(15)	0.8347(6)	0.3722(2)	0.6958(4)	5.2(2)
C(16)	0.9117(8)	0.3209(2)	0.7024(5)	9.4(4)

[a] $B(\text{eq}) = (8\pi^2/3)\sum^3_{i=1}\sum^3_{j=1}U_{ij}\mathbf{a}_i^*\mathbf{a}_j^*\vec{\mathbf{a}}_i\cdot\vec{\mathbf{a}}_j$.

collected, but it resolved to a rather high R value and so is not reported in detail (see Table 1). The main structural features are defined appropriately and agree with the proposed formula based on elemental analysis, but an exact geometry cannot be quoted at this stage.

$[Cu_2(PAP)(\mu_2\text{-}N_3)Cl_3]\cdot CH_2Cl_2$ (8). Diffraction data were collected for a dark green irregular shaped crystal of approximate dimensions 0.35 × 0.25 × 0.20 mm, in the same manner as for **1**. A summary of the crystal and other data is given in Table 1 and atomic coordinates are given in Table 4. Hydrogen atom atomic coordinates (Table S9), anisotropic thermal parameters (Table S10), a full listing of bond distances and angles (Table S11), and least-squares planes data (Table S12) are included as supplementary material.

$[Cu_2(PAP)(\mu_2\text{-}N_3)(N_3)(NO_3)(CH_3OH)](NO_3)\cdot CH_3OH$ (9). Diffraction data were collected for a green, thin platelike crystal of approximate dimensions 0.40 × 0.40 × 0.05 mm, in the same manner as for **1**. Hydrogen atoms were placed in calculated positions except for the methanol (OH) hydrogen, which was located in a difference map. All other hydrogen atoms were fixed and included in the final least squares refinement. A summary of the crystal data and other data is given in Table 1, and atomic coordinates are given in Table 5. Hydrogen atom atomic coordinates (Table S13), anisotropic thermal parameters (Table S14), a full listing of bond distances and angles (Table S15), and least-squares planes data (Table S16) are included as supplementary material.

$[Cu_2(PPD3Me)(\mu_2\text{-}N_3)Cl_3(H_2O)_{1.5}]$ (10). Diffraction data were collected for a dark, almost black, regular polyhedral crystal, of approximate dimensions 0.40 × 0.25 × 0.25 mm, in a manner similar to that for **1**. A disordered situation is apparent at some axial copper sites. O(1) and O(3) appear to be 25% occupied. Two chlorines (Cl(1) and Cl(3)) are bonded normally, but the third is bonded to either copper (Cl(2), Cl(4)), with the alternate site occupied by water. A further complication surrounds the Cl/H_2O disorder. Atoms O(2) and Cl(2) were confirmed by difference mapping, but Cl(4) could not be resolved from its alternate water molecule. In order to maintain the correct electron density Cl(4) is represented as 0.74 Cl, with 0.5 Cl/0.5 O at Cu(1). Hydrogen atoms were placed in calculated positions. A summary of the crystal and other data are given in Table 1, and

Table 3. Final Atomic Positional Parameters and B(eq) Values for $[Cu_2(DMPTD)(\mu_2\text{-}N_3)_2(N_3)_2]$ (**3**)

atom	x	y	z	B(eq)[a] (Å^2)
Cu(1)	0.2617(1)	0.0534(1)	0.4082(2)	5.2(1)
Cu(2)	0.4071(1)	0.1685(2)	0.6502(2)	5.9(1)
S(1)	−0.1121(3)	0.2960(3)	0.4521(4)	5.5(2)
S(2)	−0.0395(3)	0.4756(3)	0.7026(4)	5.4(2)
S(3)	0.1374(3)	0.5167(3)	0.9246(4)	6.0(2)
N(1)	0.178(1)	0.1073(8)	0.242(1)	4.6(7)
N(2)	0.1005(8)	0.2447(8)	0.591(1)	4.5(6)
N(3)	0.1601(8)	0.300(1)	0.707(1)	4.5(6)
N(4)	0.438(1)	0.337(1)	0.713(1)	5.3(7)
N(5)	0.357(1)	0.018(1)	0.570(1)	5.8(8)
N(6)	0.341(1)	−0.049(1)	0.645(1)	6.2(9)
N(7)	0.330(1)	−0.117(1)	0.706(2)	9(1)
N(8)	0.3562(9)	0.1823(9)	0.454(1)	4.6(6)
N(9)	0.311(1)	0.289(1)	0.434(1)	5.2(7)
N(10)	0.270(1)	0.387(1)	0.416(2)	8(1)
N(11)	0.207(1)	−0.095(1)	0.384(1)	6.3(8)
N(12)	0.199(1)	−0.169(1)	0.276(1)	5.7(8)
N(13)	0.192(1)	−0.247(1)	0.174(2)	10(1)
N(14)	0.503(2)	0.100(2)	0.798(2)	10(1)
N(15)	0.507(2)	0.139(1)	0.876(1)	4.3(7)
N(16)	0.499(4)	0.164(4)	1.008(6)	16(2)
N(16A)	0.562(3)	0.182(3)	0.976(5)	11(1)
C(1)	0.248(1)	0.114(1)	0.136(2)	5.6(9)
C(2)	0.208(1)	0.136(1)	0.013(2)	6(1)
C(3)	0.085(2)	0.159(1)	−0.009(2)	7(1)
C(4)	0.008(1)	0.154(1)	0.096(2)	5.6(9)
C(5)	0.056(1)	0.131(1)	0.222(1)	4.8(9)
C(6)	−0.027(1)	0.133(1)	0.344(1)	5.1(8)
C(7)	−0.006(1)	0.326(1)	0.578(1)	4.3(8)
C(8)	0.098(1)	0.419(1)	0.774(1)	4.8(8)
C(9)	0.296(1)	0.426(1)	0.932(1)	6(1)
C(10)	0.386(1)	0.438(1)	0.828(2)	5.0(9)
C(11)	0.411(1)	0.549(1)	0.857(2)	7(1)
C(12)	0.496(1)	0.559(1)	0.765(2)	7(1)
C(13)	0.552(1)	0.458(1)	0.652(2)	7(1)
C(14)	0.524(1)	0.349(1)	0.626(2)	6(1)

[a] See footnote *a* in Table 2.

Table 4. Final Atomic Positional Parameters and B(eq) Values for $[Cu_2(PAP)(\mu_2\text{-}N_3)Cl_3]\cdot CH_2Cl_2$ (**8**)

atom	x	y	z	B(eq)[a] Å^2
Cu(1)	0.30588(3)	0.85614(4)	−0.03840(3)	2.00(2)
Cu(2)	0.10476(3)	0.85328(5)	0.02637(3)	2.66(2)
Cl(1)	0.29510(7)	0.89385(9)	−0.17788(5)	2.58(4)
Cl(2)	−0.05651(7)	0.8745(1)	−0.06543(6)	3.46(4)
Cl(3)	0.21666(8)	0.66446(9)	−0.04952(6)	3.35(4)
Cl(4)	0.2040(1)	0.0358(1)	0.60267(7)	4.89(6)
Cl(5)	0.2695(1)	0.2167(1)	0.73137(8)	5.95(7)
N(1)	0.4561(2)	0.8125(2)	−0.0126(2)	2.0(1)
N(2)	0.5062(2)	0.9270(3)	0.1120(2)	2.3(1)
N(3)	0.3316(2)	0.8815(3)	0.0889(2)	2.0(1)
N(4)	0.2445(2)	0.8657(3)	0.1169(2)	2.1(1)
N(5)	0.1683(2)	0.8552(3)	0.2271(2)	2.2(1)
N(6)	0.0606(2)	0.7549(3)	0.1084(2)	2.5(1)
N(7)	0.1736(2)	0.9361(3)	−0.0458(2)	2.7(1)
N(8)	0.1327(2)	1.0068(3)	−0.0992(2)	2.7(1)
N(9)	0.0967(3)	1.0737(4)	−0.1488(2)	4.6(2)
C(1)	0.4861(3)	0.7486(3)	−0.0708(2)	2.8(2)
C(2)	0.5875(3)	0.7375(4)	−0.0716(3)	3.3(2)
C(3)	0.6640(3)	0.7935(4)	−0.0095(3)	3.1(2)
C(4)	0.6368(3)	0.8544(3)	0.0523(2)	2.6(2)
C(5)	0.5315(3)	0.8627(3)	0.0482(2)	2.0(1)
C(6)	0.4179(3)	0.9231(3)	0.1392(2)	1.9(1)
C(7)	0.4238(3)	0.9683(3)	0.2230(2)	2.2(1)
C(8)	0.5106(3)	1.0263(4)	0.2750(2)	2.9(2)
C(9)	0.5082(3)	1.0703(4)	0.3523(2)	3.3(2)
C(10)	0.4191(3)	1.0580(4)	0.3784(2)	3.1(2)
C(11)	0.3338(3)	1.0012(3)	0.3292(2)	2.6(2)
C(12)	0.3351(3)	0.9534(3)	0.2513(2)	1.9(1)
C(13)	0.2484(3)	0.8894(3)	0.1959(2)	1.9(1)
C(14)	0.0910(3)	0.7733(3)	0.1922(2)	2.2(1)
C(15)	0.0456(3)	0.7142(4)	0.2470(2)	2.7(2)
C(16)	−0.0283(3)	0.6324(4)	0.2145(3)	3.4(2)
C(17)	−0.0560(3)	0.6077(4)	0.1288(3)	3.7(2)
C(18)	−0.0106(3)	0.6717(4)	0.0784(2)	3.3(2)
C(19)	0.1687(4)	0.1210(4)	0.6789(3)	4.7(2)

[a] See footnote *a* in Table 2.

atomic coordinates are given in Table 6. Hydrogen atom atomic coordinates (Table S17), anisotropic thermal parameters (Table S18), a full listing of bond distances and angles (Table S19), and least-squares planes data (Table S20) are included as supplementary material.

$[Cu_2(PPD)(\mu_2\text{-}N_3)(NO_3)_3(H_2O)_{1.6}]$ (13). Diffraction data were collected for a green, irregular platelike crystal, of approximate dimensions 0.40 × 0.35 × 0.05 mm, in a manner similar to that for **1**. An empirical absorption correction was applied, after a full isotropic refinement, using DIFABS.[25] The flat and rather irregular nature of the crystal prevented the use of AGNOST. A disordered situation exists for the axial ligands with a 50:50 random mixture of nitrate and water, and a second water molecule, hydrogen bonded to the coordinated one exhibits partial occupancy (0.3). Hydrogen atoms were introduced in calculated positions, except for those in the bonded water molecule, which were located in a difference map, and all were given isotropic thermal parameters 20% greater than their bonded partners. Hydrogens in the partially occupied water were not included. A summary of the crystal and other data is given in Table 1, and atomic coordinates are given in Table 7. Hydrogen atom atomic coordinates (Table S21), anisotropic thermal parameters (Table S22), a full listing of bond distances and angles (Table S23), and least-squares planes data (Table S24) are included as supplementary material.

Results and Discussion

Description of the Structures of $[Cu_2(DMPTD)(\mu_2\text{-}N_3)(\mu_2\text{-}Cl)Cl_2]\cdot CH_3CN$ (1), $[Cu_2(DMPTD)(\mu_2\text{-}N_3)_2(N_3)_2]$ (3), $[Cu_2(DIP)(\mu_2\text{-}N_3)Cl_3]\cdot 0.5CH_3OH$ (5), $[Cu_2(PAP46Me\text{-}H)(\mu_2\text{-}N_3)(N_3)_2]\cdot 0.33H_2O$ (7), $[Cu_2(PAP)(\mu_2\text{-}N_3)Cl_3]\cdot CH_2Cl_2$ (8), $[Cu_2(PAP)(\mu_2\text{-}N_3)(N_3)(NO_3)(CH_3OH)](NO_3)\cdot CH_3OH$ (9), $[Cu_2(PPD3Me)(\mu_2\text{-}N_3)Cl_3(H_2O)_{1.5}]$ (10), $[Cu_2(PPD)(\mu_2\text{-}N_3)(NO_3)_3(H_2O)_{1.6}]$ (13). The structure of **1** is shown in Figure 2, and bond distances and angles relevant to the copper coordination spheres are given in Table 8. The two distorted square-pyramidal copper(II) centers are bridged equatorially by azido and thiadiazole groups and axially by a chlorine, and the two remaining terminal, equatorial sites at each copper are occupied by a chlorine and a pyridine. The azide bridge angle of 105.9(1)° (Cu(1)−N(5)−Cu(2)) lies at the upper limit of the range reported for bis end-on (μ_2-1,1) azido copper(II) complexes[15,16,32−34] and mixed (μ_2-1,1) azido and μ_2-hydroxo or μ_2-phenoxo-complexes,[17,35−37] and is comparable to that (105.0(8)°) observed in the analogous bromo derivative $[Cu_2(DMPTD)(\mu_2\text{-}N_3)(\mu_2\text{-}Br)Br_2]\cdot CH_3CN$ (**2**) (Figure 3).[20] The angle at the chloro bridge in **1** (77.33(4)°) is significantly larger, and the axial copper-chlorine distances are shorter than those reported for other similar (triply bridged), axially chlorine-bridged, dicopper(II) complexes involving related tetradentate (N_4) diazine ligands.[38,39] The Cu−Cu separation (3.1215(7) Å) is comparable to those observed for the bromo derivative (**2**) (3.138(3) Å)[20] and the triply bridged dinuclear copper(II) complexes $[Cu_2(PTPH)(\mu_2\text{-}Cl)_2Cl_2]\cdot 2CH_3OH$ (3.1194(2) Å)

(32) Mak, T. C. W.; Goher, M. A. S. *Inorg. Chim. Acta* **1986**, *115*, 17.
(33) Goher, M. A. S.; Mak, T. C. W. *Inorg. Chim. Acta* **1984**, *117*, 117.
(34) Mautner, F. A.; Goher, M. A. S. *Polyhedron* **1992**, *11*, 2537.
(35) Benzekri, A.; Dubourdeaux, P.; Latour, J-M.; Rey, P.; Laugier, J. *J. Chem Soc., Dalton Trans.* **1991**, 3359.
(36) Karlin, K. D.; Farooq, A.; Hayes, J. C.; Cohen, B. I.; Rowe, T. M.; Sinn, E.; Zubieta, J. *Inorg. Chem.* **1987**, *26*, 1271.
(37) Sorrell, T. N. In *Biological and Inorganic Copper Chemistry*, Karlin, K. D., Zubieta, J., Eds.; Adenine: Guilderland, NY, 1986; Vol. 2, pp 41−65 and references therein.
(38) Chen, L.; Thompson, L. K.; Bridson, J. N. *Inorg. Chim. Acta* **1993**, *214*, 67.
(39) Marongiu, G.; Lingafelter, E. C. *Acta Crystallogr.* **1982**, *B38*, 620.

Table 5. Final Atomic Positional Parameters and B(eq) Values for $[Cu_2(PAP)(\mu_2\text{-}N_3)(N_3)(NO_3)(CH_3OH)](NO_3)\cdot CH_3OH$ (**9**)

atom	x	y	z	B(eq)[a] (Å^2)
Cu(1)	0.35850(7)	0.26644(6)	0.1035(1)	2.43(6)
Cu(2)	0.62508(8)	0.12609(6)	0.2378(1)	2.65(6)
O(1)	0.2801(4)	0.2455(4)	−0.1413(5)	3.4(3)
O(2)	0.2790(5)	0.3903(4)	−0.1519(8)	6.1(5)
O(3)	0.2015(6)	0.3246(5)	−0.3796(7)	8.7(6)
O(4)	0.8284(5)	0.2858(4)	0.1729(7)	5.2(5)
O(5)	0.7576(5)	0.2090(4)	0.2753(6)	4.7(4)
O(6)	0.7561(5)	0.1906(4)	0.0053(6)	5.7(5)
O(7)	0.4084(4)	0.1041(4)	0.1667(6)	4.1(4)
O(8)	0.8663(6)	0.3501(5)	0.5212(8)	9.0(5)
N(1)	0.2102(5)	0.3311(4)	0.1714(7)	2.6(4)
N(2)	0.2682(5)	0.4439(4)	0.3710(7)	2.8(4)
N(3)	0.4343(5)	0.3031(4)	0.3392(6)	1.9(3)
N(4)	0.5488(4)	0.2370(4)	0.4022(6)	1.9(3)
N(5)	0.7158(5)	0.1880(4)	0.6258(6)	2.4(4)
N(6)	0.7225(5)	0.0434(4)	0.4447(6)	2.6(4)
N(7)	0.5088(5)	0.2142(4)	0.0528(6)	2.6(4)
N(8)	0.5152(5)	0.1960(4)	−0.0993(8)	3.2(4)
N(9)	0.5185(6)	0.1789(5)	−0.2395(8)	5.6(6)
N(10)	0.6882(5)	0.0160(4)	0.0740(7)	2.9(4)
N(11)	0.7926(7)	−0.0233(5)	0.0937(8)	4.1(5)
N(12)	0.8833(7)	−0.0667(7)	0.100(1)	9.1(8)
N(13)	0.2525(6)	0.3217(5)	−0.2284(8)	4.2(5)
N(14)	0.7812(5)	0.2287(4)	0.1509(8)	3.2(4)
C(1)	0.1298(7)	0.2958(6)	0.0949(9)	3.8(6)
C(2)	0.0218(7)	0.3422(6)	0.121(1)	4.3(6)
C(3)	−0.0082(7)	0.4293(7)	0.226(1)	4.4(6)
C(4)	0.0729(7)	0.4643(5)	0.3045(9)	3.5(5)
C(5)	0.1836(6)	0.4119(5)	0.2806(8)	2.7(5)
C(6)	0.3844(6)	0.3870(5)	0.4270(7)	2.1(4)
C(7)	0.4508(6)	0.4228(5)	0.5772(7)	1.9(4)
C(8)	0.4057(6)	0.5184(5)	0.6590(8)	2.7(4)
C(9)	0.4757(6)	0.5486(5)	0.7938(8)	2.8(5)
C(10)	0.5898(7)	0.4831(5)	0.8565(8)	2.9(5)
C(11)	0.6347(6)	0.3892(5)	0.7804(8)	2.6(4)
C(12)	0.5663(6)	0.3566(5)	0.6416(7)	2.2(4)
C(13)	0.6087(6)	0.2579(5)	0.5519(8)	1.9(4)
C(14)	0.7646(6)	0.0835(5)	0.5945(9)	2.5(4)
C(15)	0.8565(7)	0.0241(6)	0.7234(9)	3.8(5)
C(16)	0.9010(7)	−0.0775(7)	0.700(1)	4.9(6)
C(17)	0.8538(7)	−0.1217(5)	0.554(1)	4.2(5)
C(18)	0.7650(7)	−0.0590(6)	0.4288(9)	3.3(5)
C(19)	0.4000(9)	0.0824(7)	0.321(1)	6.0(8)
C(20)	0.9259(9)	0.2824(8)	0.650(1)	7.3(9)

[a] See footnote *a* in Table 2.

(PTPH = 3,6-bis(2′-pyridylthio)phthalazine)[40] and $[Cu_2(PTP)(\mu_2\text{-}Cl)_2Cl_2]$[41] (PTP = 3,6-bis(2′-pyridylthio)pyridazine). The copper−nitrogen (diazole) distances (Cu(1)−N(2) 2.198(3) Å, Cu(2)−N(3) 2.277(3) Å), which differ markedly, are quite long, but comparable to those observed for analogous dinuclear copper(II) complexes **2** (2.22(1), 2.26(1) Å) and $[Cu_2(DMPTD)(\mu_2\text{-}Cl)_2Cl_2]$ (2.21(2), 2.27(2) Å).[42] The long copper thiadiazole contacts can be attributed to the seven-membered chelate rings created by the terminal pyridine nitrogen atoms, which effectively force the thiadiazole ring away from the copper atoms. The asymmetry in the dinuclear center extends to the azide bridge, with slightly different copper−nitrogen distances (1.947(3), 1.965(3) Å) and Cu−N−N angles (126.1(3), 127.6(3)°). The sum of the angles at N(5) (359.6°) is indicative of a planar arrangement around the bridging azide nitrogen atom. Cu(1) and Cu(2) are displaced by 0.463(3) and 0.567(3) Å from the mean planes of the four in-plane donors N(1), N(2), N(5), Cl(2) and N(3), N(4), N(5), Cl(3), respectively (toward Cl(1)). The two mean planes are mutually inclined by 48.43°. The pyridine ring mean planes defined by N(1) and N(4) are inclined by 137.51 and 111.81°, respectively, relative to the mean thiadiazole plane.

The structure of **3** is illustrated in Figure 4, and bond distances and angles relevant to the copper coordination spheres are given in Table 9. The two copper centers have essentially square-planar stereochemistries with four in-plane nitrogen donors. Two azide groups act as μ_2-1,1-bridges, and the other terminal sites are occupied by a pyridine nitrogen and a terminal azide at Cu-

Table 6. Final Atomic Positional Parameters and B(eq) Values for $[Cu_2(PPD3Me)(\mu_2\text{-}N_3)Cl_3(H_2O)_{1.5}]$ (**10**)

atom	x	y	z	B(eq)[a] (Å^2)
Cu(1)	0.72963(7)	0.05827(7)	0.29269(6)	3.12(4)
Cu(2)	1.03172(7)	0.14903(7)	0.28458(5)	2.84(4)
Cl(1)	0.6033(2)	−0.0131(2)	0.1703(1)	3.96(8)
Cl(2)	0.827(1)	−0.0946(9)	0.4094(7)	4.2(3)
Cl(3)	1.1225(2)	0.1154(2)	0.1666(1)	3.99(9)
Cl(4)	1.1197(3)	0.0004(3)	0.4036(2)	6.3(2)
O(1)	0.657(3)	0.274(3)	0.201(2)	14(2)
O(2)	0.823(3)	−0.098(3)	0.381(1)	6(1)
O(3)	0.901(2)	0.289(2)	0.181(1)	6(1)
N(1)	0.6002(5)	0.0918(4)	0.3694(4)	2.9(2)
N(2)	0.6420(4)	0.1658(4)	0.4383(3)	2.7(2)
N(3)	0.8204(4)	0.1688(4)	0.3817(3)	2.4(2)
N(4)	0.9365(4)	0.2011(4)	0.3798(3)	2.3(2)
N(5)	1.1110(5)	0.2990(4)	0.4294(3)	2.6(2)
N(6)	1.1506(5)	0.2623(4)	0.3523(3)	2.6(2)
N(7)	0.8787(5)	0.0632(5)	0.2353(4)	3.1(2)
N(8)	0.8840(5)	−0.0038(5)	0.1732(4)	3.6(3)
N(9)	0.8858(6)	−0.0637(6)	0.1157(5)	5.4(4)
C(1)	0.4067(7)	−0.0128(7)	0.3203(5)	5.1(4)
C(2)	0.4849(6)	0.0659(6)	0.3800(5)	3.2(3)
C(3)	0.4547(6)	0.1218(6)	0.4540(5)	3.3(3)
C(4)	0.5541(6)	0.1838(6)	0.4899(5)	3.3(3)
C(5)	0.7633(6)	0.2066(5)	0.4458(4)	2.5(3)
C(6)	0.8197(6)	0.2775(5)	0.5141(4)	2.7(3)
C(7)	0.9366(6)	0.3094(5)	0.5129(4)	3.0(3)
C(8)	0.9935(6)	0.2700(5)	0.4431(4)	2.3(3)
C(9)	1.1933(6)	0.3694(6)	0.4781(5)	3.4(3)
C(10)	1.2891(6)	0.3785(6)	0.4309(5)	3.6(3)
C(11)	1.2594(6)	0.3114(5)	0.3528(4)	2.8(3)
C(12)	1.3338(6)	0.2990(6)	0.2801(5)	4.1(4)

[a] See footnote *a* in Table 2.

Table 7. Final Atomic Positional Parameters and B(eq) Values for $[Cu_2(PPD)(\mu_2\text{-}N_3)(NO_3)_3(H_2O)_{1.6}]$ (**13**)

atom	x	y	z	B(eq)[a] (Å^2)
Cu(1)	0.4046(2)	0.16771(7)	0.6846(2)	2.36(5)
O(1)	0.540(1)	0.1126(4)	0.909(1)	3.3(3)
O(2)	0.473(2)	0.0589(5)	1.121(1)	7.0(5)
O(3)	0.231(1)	0.1179(4)	0.910(1)	4.5(4)
O(4)	0.710(3)	0.1894(8)	0.656(2)	2.7(4)
O(5)	0.746(5)	0.129(2)	0.488(5)	8(1)
O(6)	0.905(3)	0.213(1)	0.555(3)	7.7(5)
O(7)	0.725(3)	0.166(1)	0.681(2)	3.4(4)
O(8)	0.81(1)	0.130(4)	0.49(1)	10(2)
N(1)	0.269(1)	0.0979(4)	0.490(1)	2.3(4)
N(2)	0.135(1)	0.1208(4)	0.313(1)	2.4(3)
N(3)	0.246(1)	0.2186(4)	0.444(1)	2.1(3)
N(4)	0.448(2)	1/4	0.828(1)	2.0(4)
N(5)	0.469(2)	1/4	0.998(2)	2.6(5)
N(6)	0.489(2)	1/4	1.154(2)	5.0(8)
N(7)	0.410(2)	0.0956(5)	0.984(1)	3.8(5)
N(8)	0.795(3)	0.162(1)	0.563(2)	2.6(3)
C(1)	0.243(2)	0.0373(5)	0.481(2)	3.1(5)
C(2)	0.090(2)	0.0171(6)	0.297(2)	4.1(6)
C(3)	0.026(2)	0.0716(6)	0.200(1)	3.4(5)
C(4)	0.124(1)	0.1867(5)	0.288(1)	2.2(4)
C(5)	−0.004(1)	0.2174(5)	0.115(1)	3.1(4)

[a] See footnote *a* in Table 2.

(40) Chen, L.; Thompson, L. K.; Bridson, J. N. *Inorg. Chem.* **1993**, *32*, 2938.
(41) Mandal, S. K.; Thompson, L. K.; Newlands, M. J.; Lee, F. L.; LePage, Y.; Gabe, E. J. *Inorg. Chim. Acta* **1986**, *122*, 199.
(42) Tandon, S. S.; Chen, L.; Thompson, L. K.; Bridson, J. N. *Inorg. Chem.* **1994**, *33*, 490.

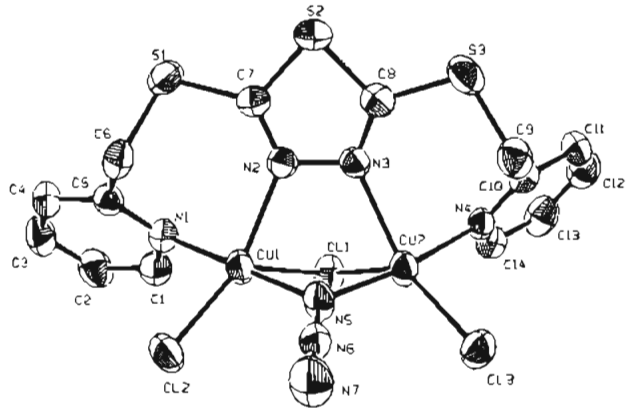

Figure 2. Structural representation of $[Cu_2(DMPTD)(\mu_2\text{-}N_3)(\mu_2\text{-}Cl)Cl_2]$ (**1**) with hydrogen atoms omitted (50% probability thermal ellipsoids).

Table 8. Interatomic Distances (Å) and Angles (deg) Relevant to the Copper Coordination Spheres in $[Cu_2(DMPTD)(\mu_2\text{-}N)(\mu_2\text{-}Cl)Cl_2]\cdot CH_3CN$ (**1**)

Cu(1)−Cl(1)	2.519(1)	Cu(1)−Cl(2)	2.253(1)
Cu(1)−N(1)	1.997(3)	Cu(1)−N(2)	2.198(3)
Cu(1)−N(5)	1.965(3)	Cu(2)−Cl(1)	2.477(1)
Cu(2)−Cl(3)	2.258(1)	Cu(2)−N(3)	2.277(3)
Cu(2)−N(4)	1.986(3)	Cu(2)−N(5)	1.947(3)
Cu(2)−Cu(2)	3.1215(7)		
Cl(1)−Cu(1)−Cl(2)	128.57(5)	Cl(1)−Cu(1)−N(1)	96.71(9)
Cu(1)−N(2)−N(3)	113.4(2)	Cl(1)−Cu(1)−N(2)	86.29(8)
Cl(1)−Cu(1)−N(5)	82.7(1)	N(1)−Cu(1)−N(5)	179.0(1)
Cl(2)−Cu(1)−N(1)	88.00(8)	Cu(2)−N(3)−N(2)	111.3(2)
Cl(2)−Cu(1)−N(2)	144.26(8)	Cl(2)−Cu(1)−N(5)	91.83(9)
N(1)−Cu(1)−N(2)	96.2(1)	Cl(3)−Cu(2)−N(4)	92.66(8)
N(2)−Cu(1)−N(5)	84.5(1)	Cl(1)−Cu(2)−Cl(3)	132.31(4)
Cu(1)−N(5)−Cu(2)	105.9(1)	Cl(1)−Cu(2)−N(3)	89.25(8)
Cu(1)−N(5)−N(6)	126.1(3)	Cl(1)−Cu(2)−N(4)	93.95(9)
Cu(2)−N(5)−N(6)	127.6(3)	Cl(1)−Cu(2)−N(5)	84.2(1)
Cl(3)−Cu(2)−N(3)	137.69(8)	N(3)−Cu(2)−N(4)	91.6(1)
Cl(3)−Cu(2)−N(5)	94.39(9)	N(4)−Cu(2)−N(5)	172.0(1)
N(3)−Cu(2)−N(5)	80.5(1)		
Cu(1)−Cl(1)−Cu(2)	77.33(4)		

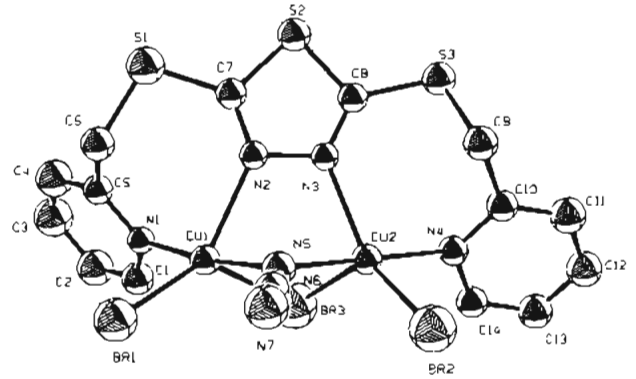

Figure 3. Structural representation of $[Cu_2(DMPTD)(\mu_2\text{-}N_3)(\mu_2\text{-}Br)Br_2]$ (**2**) with hydrogen atoms omitted (50% probability thermal ellipsoids).

(1), and a pyridine nitrogen and a disordered "wagging" azide at Cu(2). The ligand wraps itself around the dinuclear center in **3** in such a way that the thiadiazole nitrogen atoms are poised above the copper centers in pseudoaxial positions. The Cu(1)−N(2) and Cu(2)−N(3) distances exceed 2.53 Å, and so are considered as weak contacts. This contrasts sharply with the situation in **1** and **2**, where these donor atoms occupy equatorial sites. This is again seen as a direct consequence of the ligand bite and the formation of the seven membered chelate rings. In plane contacts to the bridging azides are short (<2.05 Å), and

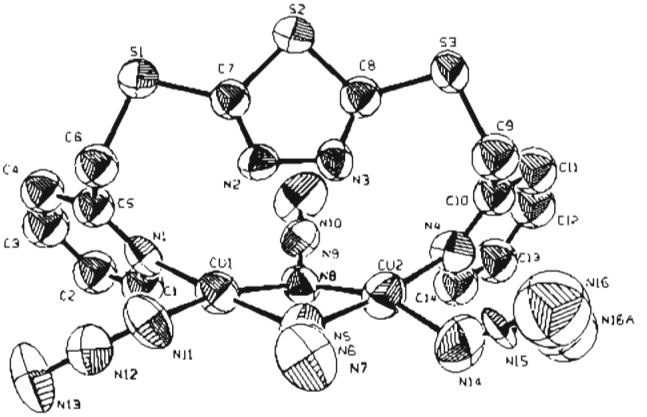

Figure 4. Structural representation of $[Cu_2(DMPTD)(\mu_2\text{-}N_3)_2(N_3)_2]$ (**3**) with hydrogen atoms omitted (50% probability thermal ellipsoids).

Table 9. Intramolecular Distances (Å) and Angles (deg) Relevant to the Copper Coordination Spheres in $[Cu_2(DMPTD)(\mu_2\text{-}N_3)_2(N_3)_2]$ (**3**)

Cu(1)−N(1)	2.014(8)	Cu(2)−O(1)	1.938
Cu(1)−N(5)	2.043(9)	Cu(2)−N(4)	1.998(9)
Cu(1)−N(8)	1.995(9)	Cu(2)−N(5)	2.022(9)
Cu(1)−N(11)	1.94(1)	Cu(2)−N(8)	1.966(9)
Cu(1)−N(2)	2.538(8)	Cu(2)−N(3)	2.680(8)
Cu(1)−Cu(2)	3.076(2)		
N(1)−Cu(1)−N(5)	95.0(4)	Cu(1)−N(5)−Cu(2)	98.3(4)
N(1)−Cu(1)−N(8)	172.0(4)	Cu(1)−N(5)−N(6)	121.8(7)
N(1)−Cu(1)−N(11)	97.4(4)	Cu(2)−N(5)−N(6)	120.3(7)
N(5)−Cu(1)−N(8)	77.1(4)	N(5)−N(6)−N(7)	180(1)
N(5)−Cu(1)−N(11)	165.7(4)	Cu(1)−N(8)−Cu(2)	101.9(4)
N(8)−Cu(1)−N(11)	90.3(4)	Cu(1)−N(8)−N(9)	125.4(8)
O(1)−Cu(2)−N(4)	95.1	Cu(2)−N(8)−N(9)	126.0(8)
O(1)−Cu(2)−N(5)	153.4	N(8)−N(9)−N(10)	177(1)
O(1)−Cu(2)−N(8)	92.8	N(11)−N(12)−N(13)	175(1)
N(4)−Cu(2)−N(5)	94.8(4)		
N(4)−Cu(2)−N(8)	172.1(3)		
N(5)−Cu(2)−N(8)	78.3(4)		
Cu(1)−N(11)−N(12)	127(1)		

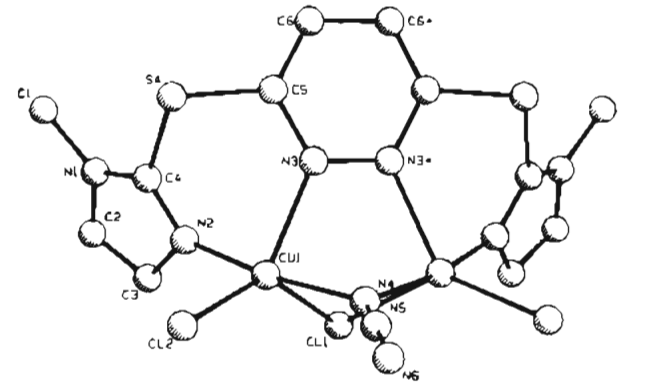

Figure 5. Structural representation of $[Cu_2(DIP)(\mu_2\text{-}N_3)(\mu_2\text{-}Cl)Cl_2]$ (**5**).

the two N_4 least squares-planes are bent slightly about an axis joining the azide nitrogens N(5) and N(8), with a dihedral angle of 17.8°. The mean planes of the pyridine rings defined by N(1) and N(4) are inclined by 104.3 and 102.7°, respectively, relative to the thiadiazole mean plane. The fact that the two bridging azides occupy equatorial sites leads to a situation where the azide bridge angles (98.3(4), 101.9(2)°) are much smaller than that in **1** (105.9(1)°), and the copper−copper separation is somewhat smaller (Cu(1)−Cu(2) 3.076(2) Å).

The preliminary structure of **5** is illustrated in Figure 5. The two copper(II) centers are bridged by three groups, the pyridazine N_2, a μ_2-1,1-azide, and a chlorine. The geometry at copper is highly distorted but, despite a Cl(2)−Cu(1)−N(3)

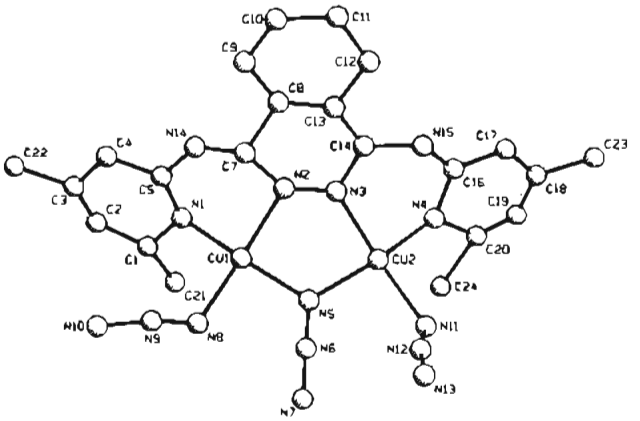

Figure 6. Structural representation of $[Cu_2(PAP46Me\text{-}H)(\mu_2\text{-}N_3)(N_3)_2]$ (**7**).

angle of 129.5(7)°, is better described as a distorted square-pyramid, rather than a trigonal bipyramid (N(2)−Cu(1)−N(4) 170(1)°, N(3)−Cu(1)−Cl(1) 94.4(6)°, N(3)−Cu(1)−N(4) 86-(1)°). The bridging chlorine therefore occupies an axial site, while, as usual, the azide bridges in an equatorial position. Copper−nitrogen distances to N(2) and N(4) are short (1.91(2) and 1.97(2) Å, respectively), while the Cu(1)−N(3) distance is somewhat longer (2.15(2) Å). The ligand DIP resembles PAP, PTP, and PTPH, all of which combine a six-membered diazine ring and six-membered chelate rings. The azide bridge angle of 101(2)° is consistent with hydroxide bridge angles in related triply bridged PAP, PTP, and PTPH complexes, which fall in the range 100−106.2°.[38,39,43] The ligand is twisted in a symmetric fashion creating a plane of symmetry, which passes through the bridging azide and chloride. The imidazole mean planes are inclined by an angle of 53.6° relative to the pyridazine mean plane.

Azide displaces hydroxide in the reaction that produces compound **7** and occupies a bridge position typical of hydroxide in other systems. The preliminary structural refinement of **7** reveals two main fragments, which are two slightly different dinuclear complexes, both involving tetradentate ligands and essentially planar copper centers with just phthalazine and μ_2-1,1-azide bridges, and one terminally bound azide per copper (Figure 6 illustrates one). The in-plane contacts are short with Cu-N distances < 2.1 Å. The consequence of two groups bridging the copper centers is to create a very large Cu−N(azide)−Cu angle, which exceeds 116° (Cu(1)−Cu(2) 3.328-(7) Å), and is a most unusual structural feature for azide complexes. The analytical data for compound **7** indicates only three azides per dinuclear unit, and as a consequence the ligand must be acting as an anion, having lost an NH proton. The structural data for **7** are not well enough resolved to reveal the site of deprotonation, but the absence of any lattice fragments that could be associated with an anionic group support the analytical data.

The structure of **8** is illustrated in Figure 7, and bond distances and angles relevant to the copper coordination spheres are given in Table 10. A square-planar copper and a square-pyramidal copper center are bridged by the phthalazine diazine and a μ_2-1,1-azide, with an axial chlorine, (Cl(3)), bonded to Cu(1) (Cu-(1)−Cl(3) 2.491(2) Å). This chlorine does not play a strong bridging role between the two copper centers (Cu(2)−Cl(3) 3.097(2) Å), but because of the relatively short Cu−Cu separation (3.1649(8) Å), compared with **7**, there may be some bridging contact. The azide bridge angle is 107.9(2)°, and the

(43) Chen, L.; Thompson, L. K.; Bridson, J. N. Unpublished results.

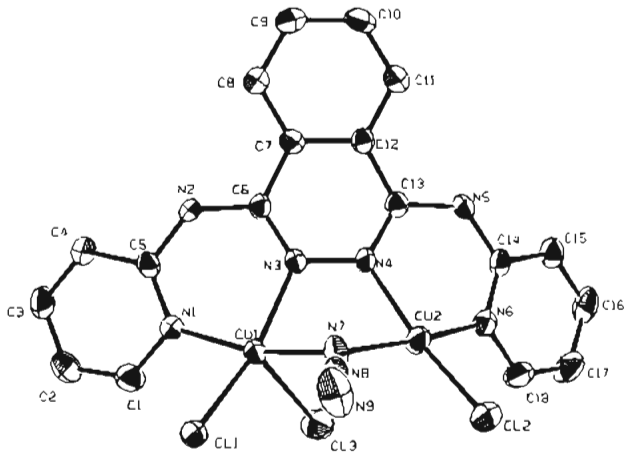

Figure 7. Structural representation of $[Cu_2(PAP)(\mu_2\text{-}N_3)Cl_3]$ (**8**) with hydrogen atoms omitted (50% probability thermal ellipsoids).

Table 10. Intramolecular Distances (Å) and Angles (deg) Relevant to the Copper Coordination Spheres in $[Cu_2(PAP)(\mu_2\text{-}N_3)Cl_3]\cdot CH_2Cl_2$ (**8**)

Cu(1)−Cl(1)	2.295(1)	Cu(2)−Cl(2)	2.264(1)
Cu(1)−Cl(3)	2.491(2)	Cu(2)−N(4)	2.034(3)
Cu(1)−N(1)	1.996(3)	Cu(2)−N(6)	1.976(3)
Cu(1)−N(3)	2.040(3)	Cu(2)−N(7)	1.946(3)
Cu(1)−N(7)	1.968(3)	Cu(1)−Cu(2)	3.1649(8)
Cl(1)−Cu(1)−Cl(3)	101.70(4)	Cu(1)−N(7)−Cu(2)	107.9(2)
Cl(1)−Cu(1)−N(1)	91.76(8)	Cu(1)−N(7)−N(8)	124.9(2)
Cl(1)−Cu(1)−N(3)	159.98(9)	Cu(2)−N(7)−N(8)	125.3(2)
Cl(1)−Cu(1)−N(7)	92.98(9)	N(7)−N(8)−N(9)	178.5(4)
Cl(3)−Cu(1)−N(1)	103.00(9)	Cl(2)−Cu(2)−N(4)	168.76(9)
Cl(3)−Cu(1)−N(3)	97.97(9)	Cl(2)−Cu(2)−N(6)	95.84(9)
Cl(3)−Cu(1)−N(7)	90.4(1)	Cl(2)−Cu(2)−N(7)	93.96(9)
N(1)−Cu(1)−N(3)	87.4(1)	N(4)−Cu(2)−N(6)	86.2(1)
N(1)−Cu(1)−N(7)	164.6(1)	N(4)−Cu(2)−N(7)	85.1(1)
N(3)−Cu(1)−N(7)	83.1(1)	N(6)−Cu(2)−N(7)	169.2(1)
Cu(1)−N(3)−N(4)	114.3(2)	Cu(2)−N(4)−N(3)	116.8(2)

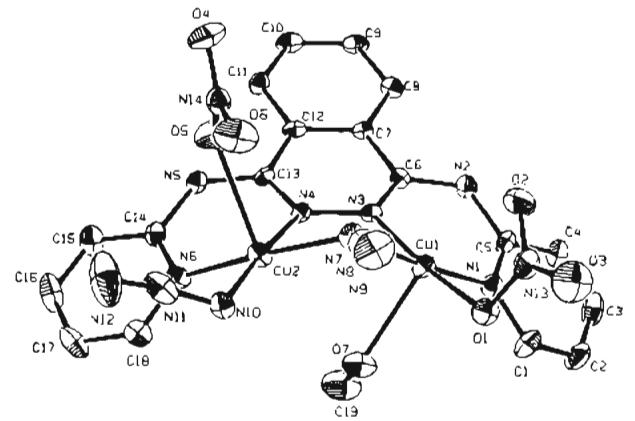

Figure 8. Structural representation of $[Cu_2(PAP)(\mu_2\text{-}N_3)(N_3)(NO_3)(CH_3OH)]^+$ (**9**) with hydrogen atoms omitted (50% probability thermal ellipsoids).

sum of the angles around N(7) (358.1°) indicates essential planarity at the bridgehead nitrogen. In-plane copper−nitrogen distances are normal, and the copper least-squares basal N_4 planes are mutually inclined by 135.9°. The absence of a true chlorine bridge leads to a flattening of the whole molecule and the pyridine mean planes defined by N(1) and N(6) are inclined by 21.7 and 32.6°, respectively, relative to the mean phthalazine plane.

The structure of **9** is illustrated in Figure 8, and bond distances and angles relevant to the copper coordination spheres are given in Table 11. The two copper centers are bridged equatorially by the phthalazine diazine and a μ_2-1,1-azide, with a terminal

Table 11. Intramolecular Distances (Å) and Angles (deg) Relevant to the Copper Coordination Spheres in $[Cu_2(PAP)(\mu_2\text{-}N_3)(N_3)(NO_3)(CH_3OH)](NO_3)\cdot CH_3OH$ (**9**)

Cu(1)−O(1)	1.993(4)	N(7)−N(8)	1.234(7)
Cu(1)−N(1)	1.990(6)	N(8)−N(9)	1.129(7)
Cu(1)−N(3)	1.990(5)	N(10)−N(11)	1.224(8)
Cu(1)−N(7)	1.959(6)	N(11)−N(12)	1.084(9)
Cu(1)−O(7)	2.303(5)	Cu(2)−N(7)	1.954(5)
Cu(2)−N(4)	2.019(5)	Cu(2)−N(10)	1.957(5)
Cu(2)−N(6)	1.989(5)	Cu(1)−Cu(2)	3.177(2)
O(1)−Cu(1)−N(1)	91.6(2)	Cu(1)−N(3)−N(4)	115.2(4)
O(1)−Cu(1)−N(3)	173.1(2)	Cu(1)−N(7)−Cu(2)	108.6(2)
O(1)−Cu(1)−N(7)	93.2(2)	Cu(1)−N(7)−N(8)	119.3(5)
N(1)−Cu(1)−N(3)	88.7(2)	Cu(2)−N(7)−N(8)	121.6(5)
N(1)−Cu(1)−N(7)	173.7(2)	N(7)−N(8)−N(9)	178.2(8)
N(3)−Cu(1)−N(7)	86.1(2)	Cu(2)−N(10)−N(11)	117.4(5)
N(4)−Cu(2)−N(6)	87.1(2)	N(10)−N(11)−N(12)	172(1)
N(4)−Cu(2)−N(7)	85.9(2)	Cu(2)−N(4)−N(3)	117.5(3)
N(4)−Cu(2)−N(10)	175.3(2)	N(6)−Cu(2)−N(10)	93.8(2)
N(6)−Cu(2)−N(7)	170.6(2)	N(7)−Cu(2)−N(10)	92.8(2)

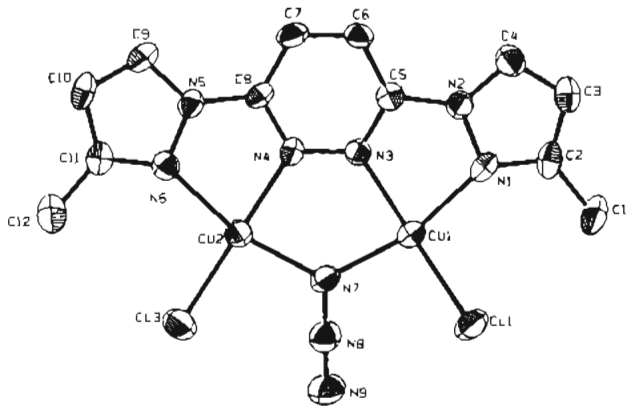

Figure 9. Structural representation of $[Cu_2(PPD3Me)(\mu_2\text{-}N_3)Cl_3(H_2O)_{1.5}]$ (**10**) with hydrogen atoms omitted (50% probability thermal ellipsoids).

azide bound to Cu(2), and a monodentate nitrate bound to Cu(1). In plane copper−ligand distances are normal. The two copper centers are separated by 3.177(2) Å, with a Cu−N−Cu angle of 108.6(3)° at the bridging azide. Cu(1) is square-pyramidal with an unusual, tightly bound methanol in the axial position (Cu(1)−O(7) 2.303(5) Å), but with a long contact to Cu(2) (2.967(7) Å). Once again the relatively small Cu−Cu separation would indicate a restraining influence on the part of the methanol and a weak bridging interaction. Cu(2) is best described as square-pyramidal, with a more distant contact to nitrate N(14) (Cu(2)−O(5) 2.515(8) Å; see Figure 8). The two copper least squares basal N_4 and N_3O planes are mutually inclined by 127.9°, which represents a significant folding of the dinuclear center. The pyridine ring mean planes defined by N(1) and N(6) are inclined by 147.2 and 152.1°, respectively, relative to the mean phthalazine plane. The sum of the angles around the bridgehead nitrogen (N(7)) of 349.7° indicates some trigonal pyramidal distortion, due, no doubt, to the folding of the copper basal planes.

The structure of **10** is illustrated in Figure 9, and bond distances and angles relevant to the copper coordination spheres are given in Table 12. Two copper(II) centers are bridged equatorially by just the pyridazine N_2 group, and a μ_2-1,1-azide, and terminal equatorial ligands include pyrazole nitrogens and chlorines, all with normal contacts. Axial sites at both coppers involve a disordered array of partial waters and partial chlorines (see Experimental Section), with relatively long contacts (Cu(2)−Cl(4) 2.606(3) Å, Cu(2)−O(3) 2.57(2) Å, Cu(1)−O(2) 2.46(3) Å, Cu(1)−Cl(2) 2.65(1) Å, Cu(1)−O(1) 3.05(4) Å). The

Table 12. Intramolecular Distances (Å) and Angles (deg) Relevant to the Copper Coordination Spheres in $[Cu_2(PPD3Me)(\mu_2\text{-}N_3)Cl_3(H_2O)_{1.5}]$ (**10**)

Cu(1)−Cl(1)	2.225(2)	N(5)−N(6)	1.374(6)
Cu(1)−N(1)	2.023(5)	N(5)−C(8)	1.386(7)
Cu(1)−N(3)	2.024(5)	N(3)−N(4)	1.336(6)
Cu(1)−N(7)	1.980(5)	N(7)−N(8)	1.252(7)
Cu(2)−Cl(3)	2.209(2)	N(8)−N(9)	1.135(7)
Cu(2)−N(4)	2.015(5)	Cu(1)−Cu(2)	3.510(1)
Cu(2)−N(6)	2.042(5)		
Cu(2)−N(7)	1.996(5)		
Cl(1)−Cu(1)−N(1)	98.6(2)	C(8)−N(5)−C(9)	128.8(6)
Cl(1)−Cu(1)−N(3)	160.5(2)	Cu(2)−N(6)−N(5)	111.3(4)
Cl(1)−Cu(1)−N(7)	95.4(2)	Cu(2)−N(6)−C(11)	143.0(4)
N(1)−Cu(1)−N(3)	78.5(2)	N(5)−N(6)−C(11)	105.6(5)
N(1)−Cu(1)−N(7)	163.4(2)	Cu(1)−N(7)−Cu(2)	124.1(3)
N(3)−Cu(1)−N(7)	85.4(2)	Cu(1)−N(7)−N(8)	117.1(4)
Cl(3)−Cu(2)−N(4)	170.4(2)	Cu(2)−N(7)−N(8)	117.9(4)
Cl(3)−Cu(2)−N(6)	100.2(1)	N(7)−N(8)−N(9)	178.1(7)
Cl(3)−Cu(2)−N(7)	94.9(2)	Cu(1)−N(1)−N(2)	112.7(4)
N(4)−Cu(2)−N(6)	78.5(2)	Cu(1)−N(1)−C(2)	142.5(5)
N(4)−Cu(2)−N(7)	85.2(2)	Cu(1)−N(3)−N(4)	122.3(4)
N(6)−Cu(2)−N(7)	162.7(2)	Cu(2)−N(4)−N(3)	122.8(4)

copper centers can therefore be regarded as essentially square-planar, and these ligands have been excluded in Figure 9. The molecule itself is almost planar with dihedral angles of 2.1 and 8.3° between the mean pyrazole ring planes defined by N(2) and N(5) and the pyridazine mean plane, respectively, and a dihedral angle of 11.8° between the N_3Cl basal mean planes. The copper−copper separation (3.510(1) Å) is very large, and is comparable with metal−metal separations in related complexes $[Cu_2(PPD)(\mu_2\text{-}OH)X_3(H_2O)]$, $\{Cu_2(MIP)(\mu_2\text{-}OH)X_3(H_2O)\}$ (X = Cl, Br),[44,45] involving similar ligands with six-membered diazine rings and five-membered chelate rings (PPD = 3,6-bis(1′-pyrazolyl)pyridazine; MIP = 1,4-bis(1′-methyl-2′-imidazolyl) phthalazine) and is a clear illustration of the role of the ligand itself in adjusting the dimensions of the dinuclear center. The consequence of the large copper−copper separation is to create larger hydroxide bridge angles for the PPD complexes (116.4−118.9°), and even larger angles for the MIP complexes (124.9−126.3°). The very large azide bridge angle in **10** (124.1(3)°) is unprecedented, is the largest on record, and is a direct consequence of the bite of PPD3Me, which causes the two copper centers to have such a large separation and indicates the similar roles of azide and hydroxide in dinuclear complexes of this sort.

Compound **13** (Figure 10) has a structure very similar to that of **10** with an essentially flat dinuclear center, a Cu−Cu separation of 3.439(2) Å, an azide bridge angle of 119.8(5)°, and Cu−N−N diazine bridge angle of 122.1(2)°. Bond distances and angles relevant to the copper coordination spheres are given in Table 13. The copper atoms have square-pyramidal geometry, with equatorial, monodentate nitrates and an axial oxygen atom which results from a 50/50 disorder of another nitrate and a water molecule. The structure in Figure 10 depicts one of these arrangements with a hydrogen-bonded interaction between nitrate oxygen O(6) and H(6*). The copper atoms are displaced by 0.105 Å from the N_3O least-squares basal donor plane, and the pyrazole rings are mutually inclined by 11.5° and inclined by 6.16° relative to the pyridazine least squares plane. The molecule has a plane of symmetry, which bisects the pyridazine ring and the μ_2-1,1-azide bridge. The overall dimensions of the dinuclear center are almost identical to those

(44) Thompson, L. K.; Hartstock, F. W.; Robichaud, P.; Hanson, A. W. *Can. J. Chem.* **1984**, *62*, 2755.
(45) Thompson, L. K.; Mandal, S. K.; Gabe, E. J.; Lee, F. L.; Addison, A. W. *Inorg. Chem.* **1987**, *26*, 657.

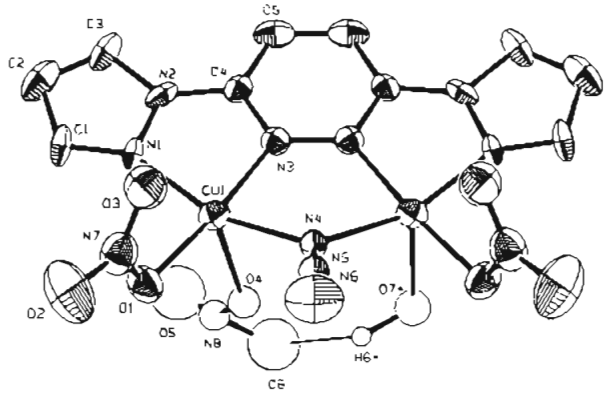

Figure 10. Structural representation of $[Cu_2(PPD)(\mu_2\text{-}N_3)(NO_3)_3(H_2O)_{1.6}]$ (**13**) with hydrogen atoms omitted (50% probability thermal ellipsoids).

Table 13. Intramolecular Distances (Å) and Angles (deg) Relevant to the Copper Coordination Spheres in $[Cu_2(PPD)(\mu_2\text{-}N_3)(NO_3)_3(H_2O)_{1.6}]$ (**13**)

Cu(1)−O(1)	1.941(7)	Cu(1)−N(1)	2.010(8)
Cu(1)−O(4)	2.27(2)	Cu(1)−N(3)	2.004(7)
Cu(1)−O(7)	2.24(2)	Cu(1)−N(4)	1.988(5)
Cu(1)−Cu(1′)	3.439(2)		
O(1)−Cu(1)−O(4)	93.8(5)	O(7)−Cu(1)−N(1)	98.5(5)
O(1)−Cu(1)−O(7)	82.7(5)	O(7)−Cu(1)−N(3)	100.2(5)
O(1)−Cu(1)−N(1)	97.0(3)	O(7)−Cu(1)−N(4)	95.4(6)
O(1)−Cu(1)−N(3)	175.0(3)	N(1)−Cu(1)−N(3)	78.6(3)
O(1)−Cu(1)−N(4)	97.3(3)	N(1)−Cu(1)−N(4)	161.2(4)
O(4)−Cu(1)−O(7)	13.3(6)	N(3)−Cu(1)−N(4)	86.5(3)
O(4)−Cu(1)−N(1)	104.6(5)	Cu(1)−N(4)−N(5)	119.6(3)
O(4)−Cu(1)−N(3)	89.6(5)	Cu(1)−N(3)−N(3)	122.1(2)
O(4)−Cu(1)−N(4)	86.7(5)	Cu(1)−N(4)−Cu(1)	119.8(5)

in $[Cu_2(PPD35Me)(\mu_2\text{-}OH)(NO_3)_2(H_2O)_2]\cdot NO_3$ (Cu−OH−Cu 119.3°, Cu−Cu 3.338(1) Å, Cu−N−N 120.0°[24]) (PPD35Me = 3,6-bis(3′,5′-dimethyl-1′-pyrazolyl)pyridazine), indicating again that the azide bridge is playing a structural role comparable to that of hydroxide, at very large bridge angles. To our knowledge the only other example of a dinuclear copper(II) center with a large μ_2-1,1-azide bridge angle, comparable to **10** and **13**, occurs in a polymeric copper(II) betaine complex, in which two copper centers are bridged by a combination of bidentate nitrate, bidentate carboxylate, and μ_2-1,1-azide, with a Cu−N_3−Cu angle of 119.5(2)°.[46]

Synthetic, Structural, and Spectroscopic Properties. Azide is a fairly strong ligand and will readily displace other ligands from the metal coordination sphere, particularly at bridging sites. However this method does not work successfully for most of the complexes under study (**1**−**6**, **8**−**13**), and they were synthesized by direct reaction of an appropriate metal salt with the ligand, in situ, followed by the addition of azide, in an appropriate solvent. Care was taken in these syntheses to avoid the addition of a large excess of sodium azide, in order to avoid the formation of explosive copper azide. For the halide complexes (**1**, **2**, **4**−**6**, **8**, **10**, **11**) the limited amount of azide added produced monosubstituted derivatives in all cases except **4**, where a diazido complex results. Halogens are reasonable ligands to copper(II), and clearly in an azide-deficient situation, limited substitution will occur. When **3**, which involved the poorer perchlorate ligand, was used and also when copper nitrate was used, complete substitution occurred, with the formation of tetraazide complexes. However, only one azide was introduced, at a bridging site, in **12** and **13**, and two were introduced in **9**.

(46) Chow, M.-Y.; Zhou, Z.-Y.; Mak, T. C. W. *Inorg. Chem.* **1992**, *31*, 4900.

Chart 1

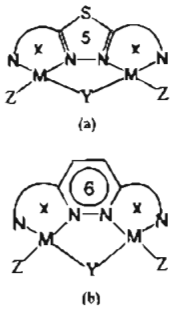

The molecular design of complexes with controlled geometric function is not a trivial matter, but can be approached by systematic adjustment of the ligand itself, particularly when many complexes within a class have been structurally characterized. The μ_2-1,2-diazine moiety is well documented as the dinucleating focus of probably hundreds of dinuclear copper, nickel, cobalt, and other metal complexes of, e.g., pyrazole, triazole, pyridazine, and phthalazine ligands.[47] Pyrazole and triazole rings are five-membered, while pyridazine and phthalazine are six-membered. The geometric consequences of these rings of different size are quite distinct (Chart 1), and lead to a situation where in the five-membered case the metal centers are further apart. For pyrazole and triazole complexes, in which the two copper centers are bonded between two tetradentate ligands, Cu−Cu separations are typically in the range 3.9−4.1 Å.[48−50] For similar dinuclear copper complexes of tetradentate pyridazine and phthalazine ligands, Cu−Cu separations are smaller in the range 3.7−3.8 Å.[51,52] In a dinuclear complex involving just one ligand, and, for example, an additional equatorial single atom bridge (Y), the M−Y−M angle would be expected to be larger for the five-membered diazine. In addition, the size of the peripheral chelate rings would be expected to influence the dinuclear center dimensions, with small rings (e.g. $x = 5$) leading to larger metal−metal separations and M−Y−M bridge angles, and vice versa. A third possible constraint would involve an axial, single or polyatomic bridge. In the case of a single atom bridge this would effectively limit the size of the dinuclear center.

DMPTD and DBITD are tetradentate N_4 ligands, and create seven-membered terminal chelate rings, which are unlikely to place great stereochemical demands on the dinuclear centers. The dimensions of the dinuclear center are therefore likely to be influenced mostly by the five-membered thiadiazole ring. In **1** and **2**, where the diazole N_2 group acts as an equatorial bridge, this leads to Cu−Cu separations in the range 3.12−3.14 Å. However in **3** the diazole ring acts as a more weakly bound, axial bridge, and the dinuclear center dimensions are influenced more strongly by the two μ_2-1,1-azide bridges, with a resulting decrease in copper−copper separation (3.076(2) Å) and Cu−N−Cu azide bridge angles. For compound **4**, with substitution of two chlorines, it would be reasonable to suggest that the azides occupy equatorial, bridging sites, and that the ligand DBITD binds in a pseudobidentate fashion, as in **3**, with

(47) Steel, P. J. *Coord. Chem. Rev.* **1990**, *106*, 227.
(48) Kamiusuki, T.; Ōkawa, H.; Matsumoto, N.; Kida, S. *J. Chem. Soc., Dalton Trans.* **1990**, 195.
(49) Bayon, J. C.; Esteban, P.; Net, G.; Rasmussen, P. G.; Baker, K. N.; Hahn, C. W.; Gumz, M. M. *Inorg. Chem.* **1991**, *30*, 2572.
(50) Koomen-van-Oudenniel, W. M. E.; de Graff, R. A. G.; Haasnoot, J. G.; Prins, R.; Reedijk, J. *Inorg. Chem.* **1989**, *28*, 1128.
(51) Tandon, S. S; Thompson, L. K.; Hynes, R. C. *Inorg. Chem.* **1992**, *31*, 2210.
(52) Abraham, F.; Lagrenee, M.; Sueur, S.; Mernari, B.; Bremard, C. *J. Chem. Soc., Dalton Trans.* **1991**, 1443.

Table 14. Magnetic and Spectral Data

complex	μ_{eff}(RT) (μ_B)	electronic spectra (nm) (ϵ = L mol^{-1} cm^{-1})	infrared spectra $\nu_{as}(N_3^-)$ (cm^{-1})
$[Cu_2(DMPTD)(\mu_2\text{-}N_3)(\mu_2\text{-}Cl)Cl_2]\cdot CH_3CN$ (**1**)	1.9	815, 740, 510, 365,[a] 820 (195), 415 (865)[b]	2083, 2057
$[Cu_2(DMPTD)(\mu_2\text{-}N_3)(\mu_2\text{-}Br)Br_2]\cdot CH_3CN$ (**2**)	1.94	950, 855, 730, 530, 350,[a] 920 (275), 810 (290), 405 (2210)[b]	2090, 2043 (sh)
$[Cu_2(DMPTD)(\mu_2\text{-}N_3)_2(N_3)_2]$ (**3**)	1.92	[935], 700, 455,[a] 735 (435), 420 (6830)[b]	2066, 2045, 2036
$[Cu_2(DBITD)(\mu_2\text{-}N_3)_2Cl_2]\cdot H_2O$ (**4**)	2.26	695, 545, 415,[a] 685 (190), 515 (350), 380 (4700)[b]	2065 (sh), 2055
$[Cu_2(DIP)(\mu_2\text{-}N_3)Cl_3]\cdot 0.5CH_3OH$ (**5**)	1.95	[900], 740, [500], [420][a]	2096
$[Cu_2(DIP)(\mu_2\text{-}N_3)Br_3]\cdot 0.5CH_3OH$ (**6**)	1.85	[865], 750, [545], [490][a]	2092
$[Cu_2(PAP46Me\text{-}H)(\mu_2\text{-}N_3)(N_3)_2]\cdot 0.33H_2O$ (**7**)	1.53	600, 430[a]	2087, 2059, 2041, 2026
$[Cu_2(PAP)(\mu_2\text{-}N_3)Cl_3]\cdot CH_2Cl_2$ (**8**)	1.58	695, [460], 360[a]	2102, 2085 (sh)
$[Cu_2(PAP)(\mu_2\text{-}N_3)(N_3)(NO_3)(CH_3OH)](NO_3)\cdot CH_3OH$ (**9**)	1.62	620, 375[a]	2096, 2052
$[Cu_2(PPD3Me)(\mu_2\text{-}N_3)Cl_3(H_2O)_{1.5}]$ (**10**)	0.49	[850], 725, 470, 410[a]	2075
$[Cu_2(PPD3Me)(\mu_2\text{-}N_3)Br_3]\cdot 0.5CH_3CN$ (**11**)	0.35	725, 490, [420][a]	2062
$[Cu_2(PPD3Me)(\mu_2\text{-}N_3)(NO_3)_3]\cdot 0.5CH_3OH$ (**12**)	1.07	690, 435[a]	2081
$[Cu_2(PPD)(\mu_2\text{-}N_3)(NO_3)_3(H_2O)_{1.6}]$ (**13**)	0.99	700, 420[a]	2087

[a] Mull transmittance. [b] DMF.

the diazole nitrogens poised above the copper axial sites. For the triply bridged DIP complex, **5** (Cu−Cu 3.036(8) Å), the ligand, which involves a six-membered diazine ring, is bound equatorially and would reasonably be expected to generate dinuclear centers with smaller Cu−Cu separations than in **1** and **2**. The analogous compound **6** presumably has the same structure. The dinuclear center in **7** involves just two bridges, and the inevitable consequence of this is for the molecule to flatten out, with concomitant increase in Cu−Cu separation and azide bridge angle. Despite the poor resolution of this structure this is shown to be the case (Cu−Cu 3.328(7) Å), Cu−N−Cu 118(2), 120(2)°). Complexes **8** and **9** both involve the same ligand (PAP), in a neutral form, but the Cu−Cu separations and Cu−N−Cu bridge angles are substantially smaller, which seems to be due to the "pseudobridging" nature of the axial chloride (**8**) and methanol (**9**), which have nominally long contacts to one copper in each case. Changing the size of the peripheral chelate ring to five, as in **10** and **13**, leads to a dramatic expansion of the dinuclear center, the overall flattening of the complex, and the largest known μ_2-1,1-azide bridge angle on record. Compounds **11** and **12** are expected to have similar structures.

Infrared absorptions associated with coordinated azide are at best difficult to interpret and rationalize. Asymmetric azide stretching vibrations occur above 2000 cm^{-1}, and the presence of more than one band is often indicative of more than one type of azide. For the complex $[Cu(2Bzpy)(N_3)_2]_2$ (2Bzpy = 2-benzylpyridine), which contains terminal azide and bridging μ_2-1,1-azides linking the coppers in an axial/equatorial combination, two strong bands are observed at 2058 and 2040 cm^{-1}, while for $[Cu(Et\text{-}nic)(N_3)_2]_n$ (Et-nic = ethyl nicotinate), which contains bridging μ_2-1,1 and μ_2-1,3 azides, two bands are also observed at 2070 (sh) and 2035 cm^{-1}.[32] The complex $[Cu_2(N_3)_2(NO_3)_2(Me_3NCH_2CO_2)_2]_n$, which contains μ_2-1,1-azide bridges, with a Cu−N−Cu angle of 119.5(2)°, exhibits ν_{as} N_3 stretching vibrations at 2101 and 2081 cm^{-1}.[46] In the complex $[Cu_2(L\text{-}O)(N_3)](PF_6)_2$, containing both equatorial phenoxide and μ_2-1,1-azide bridges,[53] a ν_{as} azide band occurs at 2068 cm^{-1}.

1 and **2** have one main absorption in this region (Table 14), resolved into two bands. The structures of these two compounds indicate just one μ_2-1,1 azide bridge, which might have suggested the appearance of just one ν_{as} azide band, but the asymmetric nature of the complexes can reasonably account for the appearance of two bands. Three well-resolved ν_{as} azide bands are observed for **3**, which has an asymmetric bis(μ_2-1,1-equatorial azide) bridge, in addition to terminal azides. The appearance of two bands for **4** would be consistent with the presence of two μ_2-1,1-azides. Compounds **5** and **6**, which have almost identical infrared spectra, each exhibit one sharp, high energy band above 2090 cm^{-1}, consistent with the structure of **5**, involving a single μ_2-1,1-azide bridge, with a plane of symmetry in the complex, which includes the azide bridge itself. Compound **7** exhibits a complex infrared spectrum in the azide region, with four clearly defined ν_{as} stretching bands. These comprise two groupings, with two high energy bands (>2058 cm^{-1}), and two bands at lower energy. In keeping with the other azide-bridged complexes the higher energy bands are associated with the μ_2-1,1-azide bridge. For compounds **8** and **10**−**13**, which involve just a single azide bridge, the high energy ν_{as} N_3 bands are clearly identified at 2062 cm^{-1} and above. For **9**, which has an azide bridge and a terminal azide, the band at 2096 cm^{-1} is assigned to the μ_2-1,1-azide, and the band at 2052 cm^{-1} to the terminal azide. These results would suggest that ν_{as} azide bands occurring above ≈2055 cm^{-1} are reasonably associated with μ_2-1,1-azide bridges.

The solid state mull transmittance electronic spectra of **1** and **2** are characterized by the presence of two to three relatively low energy d−d absorptions (Table 14) consistent with distorted square pyramidal copper ion stereochemistries, with lower energy bands for **2** consistent with the presence of coordinated bromine. Higher energy bands are associated with charge transfer transitions. The higher energy d−d absorption for **3** at 700 nm distinguishes this compound from **1** and **2**, in keeping with the pseudo-square-planar structure. A comparable single absorption for **4** at 695 nm strongly supports the proposed pseudo-square-planar structure with two in plane μ_2-1,1 azide bridges. Compounds **5** and **6** have two major d−d absorptions in the range 740−900 nm, similar to **1** and **2**, and it is reasonable to assume similar square pyramidal structures. Compound **7** exhibits one broad d−d absorption in the solid state, associated with pseudo-square-planar copper(II) centers. A much more intense band is observed at 430 nm, which is not d−d in origin, and is associated with a π−π^* ligand transition. Previous studies with neutral and anionic PAP complexes reveal a significant shift in the ligand π−π^* absorption from 338−365 nm in the neutral complexes to 391−417 nm in the anionic ones.[23] The band at 430 nm for **7** is entirely consistent with the presence of anionic PAP46Me, the slight difference in band energy being reasonably associated with the different pyridine ring substituents in this case. Visible bands at 695 and 620 nm, respectively, for **8** and **9** are consistent with the mixed pseudo-square-planar/square-pyramidal structures indicated, with higher energy π−π^* bands indicative of neutral PAP. The

(53) Karlin, K. D.; Cohen, B. I.; Hayes, J. C.; Farooq, A.; Zubieta, *J. Inorg. Chem.* **1987**, *26*, 147.

Table 15. Variable Temperature Magnetic Data

complex[a]	g	$2J$ (cm^{-1})	ϱ	TIP (10^{-6} emu)	10^2R^b	Θ (K)
$[Cu_2(DMPTD)(\mu_2\text{-}N_3)(\mu_2\text{-}Cl)Cl_2]\cdot CH_3CN$ (**1**)	2.214(1)	168(3)	0	63.4	0.17	−0.76
$[Cu_2(DMPTD)(\mu_2\text{-}N_3)(\mu_2\text{-}Br)Br_2]\cdot CH_3CN$ (**2**)	2.178(2)	118(3)	0.015	79	0.24	−1.15
$[Cu_2(DMPTD)(\mu_2\text{-}N_3)_2(N_3)_2]$ (**3**)	2.146(1)	170(2)	0	50	0.25	−2.0
$[Cu_2(DBITD)(\mu_2\text{-}N_3)_2Cl_2]\cdot H_2O$ (**4**)	2.19(1)	94(13)	0	57	0.25	0
$[Cu_2(DIP)(\mu_2\text{-}N_3)(\mu_2\text{-}Cl)Cl_2]\cdot 0.5CH_3OH$ (**5**)	2.091(3)	156(5)	0	56	0.25	−0.2
$[Cu_2(DIP)(\mu_2\text{-}N_3)(\mu_2\text{-}Br)Br_2]\cdot 0.5CH_3OH$ (**6**)	2.13(1)	60.2(6)	0	60.5	1.99	−2.2
$[Cu_2(PAP46Me\text{-}H)(\mu_2\text{-}N_3)(N_3)_2]\cdot 0.33H_2O$ (**7**)	2.05(2)	−194(4)	0.025	68	2.3	−4
$[Cu_2(PAP)(\mu_2\text{-}N_3)Cl_3]\cdot CH_2Cl_2$ (**8**)		−40[c]				
$[Cu_2(PAP)(\mu_2\text{-}N_3)(N_3)(NO_3)(CH_3OH)](NO_3)\cdot CH_3OH$ (**9**)	2.037(8)	−107(1)	0.029	83.5	2.1	−4
$[Cu_2(PPD3Me)(\mu_2\text{-}N_3)Cl_3(H_2O)_{1.5}]$ (**10**)	2.03(3)	−778(6)	0.001	73	0.69	0.9
$[Cu_2(PPD3Me)(\mu_2\text{-}N_3)Br_3]\cdot 0.5CH_3CN$ (**11**)	2.01(7)	−1092(17)	0.0004	83	1.43	0
$[Cu_2(PPD3Me)(\mu_2\text{-}N_3)(NO_3)_3]\cdot 0.5CH_3OH$ (**12**)	2.02(1)	−450(2)	0.00018	101	0.41	−5
$[Cu_2(PPD)(\mu_2\text{-}N_3)(NO_3)_3(H_2O)_{1.6}]$ (**13**)	2.030(8)	−468(2)	0.00175	51	0.42	−3

[a] In all cases, variable temperature magnetic measurements were carried out on the same, uniform, batch of complex from which crystals were chosen for structural analysis. [b] $R = [\Sigma(\chi_{obs} - \chi_{calc})^2/\Sigma(\chi_{obs})^2]^{1/2}$. [c] Estimated from χ_{max}.

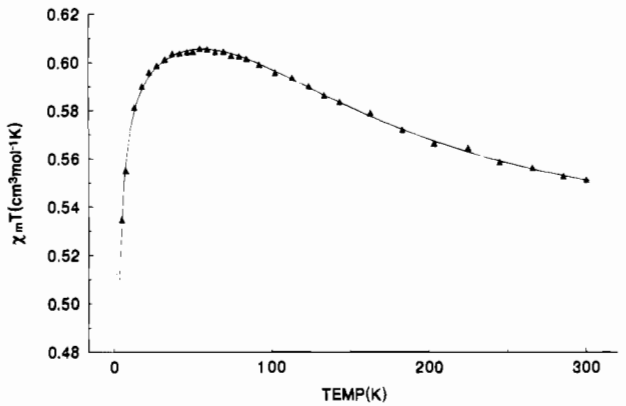

Figure 11. Plot of the magnetic data for $[Cu_2(DMPTD)(\mu_2\text{-}N_3)(\mu_2\text{-}Cl)Cl_2]\cdot CH_3CN$ (**1**). The solid line was calculated from eq 1 with g = 2.214(1), $2J$ = 168(3) cm^{-1}, ϱ = 0, $N\alpha$ = 63.4 × 10^{-6} emu, and Θ = −0.76 K (10^2R = 0.17).

additional shoulder at 460 nm in **8** is associated with halogen to metal charge transfer. Compounds **10**−**13** have visible bands in the range 690−725 nm consistent with square-pyramidal copper centers and higher energy bands associated with intraligand and ligand to metal charge transfer.

Magnetic Susceptibility Studies. Room temperature magnetic moments (μ_{eff}) for **1**−**6** (Table 14) fall in the range 1.85−2.26 μ_B (300 K), which is substantially higher than the value expected for uncoupled copper(II) ions and is indicative of the presence of ferromagnetic intradimer interactions. In sharp contrast, compounds **7**−**13** have subnormal room temperature moments indicative of antiferromagnetic coupling. Variable temperature magnetic studies (4−300 K) were carried out on powdered samples of all of the complexes. Compounds **1**−**6** show behavior typical of ferromagnetic coupling, with χ_mT versus T (K) profiles which involve an increase in χ_mT as temperature is lowered, followed by a rapid drop at low temperatures (<50 K). A typical plot is shown in Figure 11 for compound **1**. χ_mT increases from a value of 0.55 cm^3 mol^{-1} K at 300 K, reaches a maximum of approximately 0.605 cm^3 mol^{-1} K at about 80 K, remains roughly constant down to about 40 K and then drops to a value of 0.53 cm^3 mol^{-1} K at 4 K. This profile is typical of ferromagnetic coupling, with substantial stabilization of the triplet ground state.[16] The drop in χ_mT below 50 K suggests the presence of a weak intermolecular antiferromagnetic interaction, which can be accounted for by a Weiss-type correction (Θ). The theoretical expression for the magnetic susceptibility of a copper(II) dimer is given by eq 1,[54] where N, β, and k have their usual meaning, $N\alpha$ is the temperature

$$\chi_m = \frac{N\beta^2g^2}{3k(T-\Theta)}[1 + {}^1/_3\exp(-2J/kT)]^{-1}(1-\varrho) + \frac{[N\beta^2g^2]\varrho}{4kT} + N\alpha \quad (1)$$

independent paramagnetism, ϱ represents the fraction of a possible magnetically dilute impurity, and χ_m is expressed per mole of copper metal. The parameters giving the best fit for **1** were obtained using a nonlinear regression analysis with g, J, ϱ, and Θ as variables. The results of the best fit for **1** are shown as the solid line in Figure 11 with g = 2.214(1), $2J$ = 168(3) cm^{-1}, ϱ = 0, $N\alpha$ = 63.4 × 10^{-6} emu, and Θ = −0.76 K. The agreement factor 10^2R is very small, indicating a very good data fit and strong ferromagnetic coupling. The plateau of the χ_mT vs T plot in the range 40−80 K (0.605 cm^3 mol^{-1} K) may be considered to represent a situation where the excited state singlet is entirely depopulated and corresponds to a Curie law situation for the triplet state ($\chi_mT = N\beta^2g^2/3k$). An average g value calculated from this expression (2.198) corresponds very closely to that obtained from the nonlinear regression analysis, adding substantial strength to the use of this procedure for a realistic evaluation of the exchange integral. Similar analyses were carried out for compounds **2**−**6**, and the best fit parameters are given in Table 15. Very good data fits were obtained in all cases except **6**, with $2J$ values exceeding 60 cm^{-1}. In all cases spin coupling between the μ_2-1,1-azide-bridged dicopper(II) centers is dominated by ferromagnetic exchange. Small negative Weiss-like corrections were necessary for good data fits for all compounds, consistent with the drop in χ_mT at low temperatures.

Room temperature magnetic moments for **7**−**13** are subnormal (<1.65 μ_B) at room temperature, indicative of net antiferromagnetism, and for **10**−**13** the coupling is clearly very strong. Plots of χ_m vs T for all compounds show either pronounced maxima (χ_{max}) in the temperature range 30−200 K (**8** (≈30 K), **9** (≈90 K), **7** (≈170 K)) or a rising susceptibility at high temperatures approaching a maximum in χ (>300 K). An increase in susceptibility at low temperatures, in all cases, indicates the presence of small amounts of magnetically dilute paramagnetic impurities. Nonlinear regression analyses of the variable temperature (4−300 K) susceptibility data for compounds **7**−**13** were attempted using the Bleaney−Bowers equation (eq 1). Good data fits were obtained for complexes **10**−**13**, with $-2J$ values exceeding 450 cm^{-1} (Table 15). A plot of the experimental data for **10** and the theoretical line calculated with g = 2.03(3), $2J$ = −778(6) cm^{-1}, ϱ = 0.001, $N\alpha$ = 73 × 10^{-6} emu, Θ = 0.9 K, and 10^2R = 0.69, is illustrated in Figure 12. A similar plot for **13** with g = 2.030(8), $2J$ = −468(2) cm^{-1}, ϱ = 0.00175, $N\alpha$ = 51 × 10^{-6} emu, Θ = −3 K, and 10^2R = 0.42 is given in Figure 13. Compound

(54) Bleaney, B.; Bowers, K. D. *Proc. R. Soc. London* **1952**, *A214*, 451.

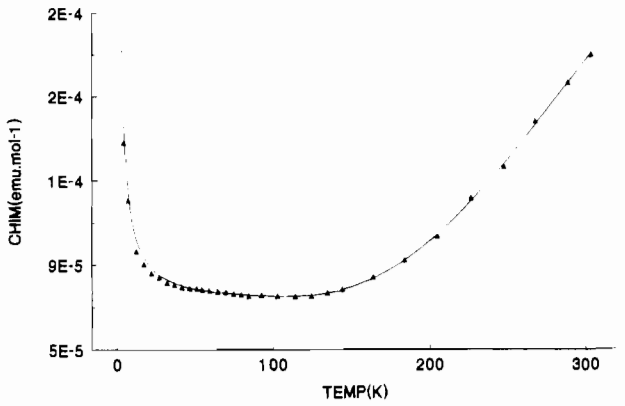

Figure 12. Plot of the magnetic data for $[Cu_2(PPD3Me)(\mu_2\text{-}N_3)Cl_3\text{-}(H_2O)_{1.5}]$ (**10**). The solid line was calculated from eq 1 with $g = 2.03\text{-}(3)$, $2J = -778(6)$ cm^{-1}, $\varrho = 0.001$, $N\alpha = 73 \times 10^{-6}$ emu, and $\Theta = 0.9$ K ($10^2R = 0.69$).

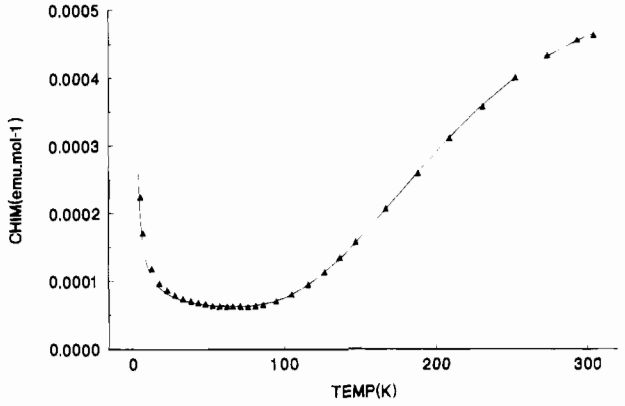

Figure 13. Plot of the magnetic data for $[Cu_2(PPD)(\mu_2\text{-}N_3)(NO_3)_3\text{-}(H_2O)_{1.6}]$ (**13**). The solid line was calculated from eq 1 with $g = 2.030\text{-}(8)$, $2J = -468(2)$ cm^{-1}, $\varrho = 0.00175$, $N\alpha = 51 \times 10^{-6}$ emu, and $\Theta = -3$ K ($10^2R = 0.42$).

11 is the most strongly coupled in the group, and based on an essentially identical infrared spectrum to that of **10** is assumed to have a similar structure, possibly with a larger azide bridge angle. We await structural data on this compound. The much smaller values of $-2J$ for **12** and **13** suggest a significant structural modification compared with **10** and **11**, and on the basis of the structure of **13**, the shorter Cu−Cu separation and the smaller azide bridge angle would be expected to be major factors.

Fitting of the variable temperature magnetic data for **7** and **9** to the Bleaney−Bowers expression gave exchange integrals of $2J = -194(4)$ and $-107(1)$ cm^{-1} respectively (Table 15). Given the large azide bridge angles in **7**, a larger exchange integral might be expected. However, the fact that the ligand (PAP46Me) is an anion, with additional negative charge, part of which is likely to be delocalized within the diazine ring, will reasonably lead to reduced antiferromagnetic coupling. Fitting of the variable temperature magnetic data for compound **8**, which had a χ_{max} value at ≈30 K, to eq 1 proved to be impossible unless unusually large Θ values are used (<-150 K). Normally Θ corrections are small, and are consistent with weak intermolecular associative effects. Since no such effects were likely for **8**, based on the X-ray structure, the large Θ value was initially regarded as anomalous. However the bulk X-ray sample was uniform and elemental analysis was entirely consistent with the structural data. A repeat of the variable temperature magnetic data gave consistent results, indicating no experimental anomalies. Regardless of the lack of an appropriate data fit using eq 1, the χ_{max} value suggests that the magnetic properties of **8** are dominated by an antiferromagnetic component with a $-2J$ value of <50 cm^{-1}. Further studies on the magnetic properties of this compound, in terms of an appropriate magnetic model, are being carried out. For all these compounds the exchange interaction between the two copper centers is propagated by two different, magnetically active bridges, the azide and the diazine. Therefore the experimentally determined $2J$ values should technically be regarded as the combined effect of these bridges, which, if considered separately would lead to quite different exchange characteristics.

For **1** and **2**, assuming a $d_{x^2-y^2}$ copper ion ground state, the axial, orthogonal halogens are not likely to contribute significantly to the total exchange, and so only the azide and diazole bridges need be considered. In a magnetostructural study involving $[Cu_2(DMPTD)(\mu_2\text{-}Cl)_2Cl_2]$ and $[Cu_2(DPTD)(\mu_2\text{-}X)_2X_2]$ (X = Cl, Br),[42] (DPTD = 2,5-bis(pyridylthio)thiadiazole), all of which involve orthogonal halogen bridging interactions, the net exchange is weakly antiferromagnetic with $-2J$ < 70 cm^{-1}, attributable to the thiadiazole bridge. For compounds **1** and **2**, which involve equatorial thiadiazole bridges (Figures 2 and 3), despite quite long Cu−N(diazole) distances (>2.198 Å), a small antiferromagnetic contribution to total exchange may be expected. Therefore the net ferromagnetism observed for both compounds highlights the dominant ferromagnetic effect associated with the μ_2-1,1-azide bridge, which is still operative for Cu−N−Cu angles of 105.9(1)° (**1**) and 105.0(8)° (**2**). Compound **3** has a very different structure with two equatorial μ_2-1,1-azide bridges, and insignificant axial contacts to the diazole nitrogen pair (Cu(1)−N(2) 2.579(9) Å, Cu(2)−N(3) 2.730(9) Å). Spin coupling in this case can therefore be assigned unequivocally to the bridging azides. The azide bridge angles of 98.1(4) and 104.1(5)° are consistent with earlier ferromagnetic complexes.[15,16] Compound **5** falls nicely in the ferromagnetic realm with an azide angle of 101(2)°. The pyridazine bridge itself is expected to propagate antiferromagnetic exchange. For the complex $[Cu_2(PTP)Cl_4]$, involving just a magnetically active pyridazine bridge between $d_{x^2-y^2}$ copper centers and with an average Cu−N−N(diazine) bridge angle of 117.0°, $2J = -131$ cm^{-1}.[55] The smaller Cu−N−N angle of 113.1(6)° found in **5** perhaps would suggest a weaker antiferromagnetic effect through the diazine bridge. Regardless, the ferromagnetic contribution associated with the azide bridge far outweighs the antiferromagnetic coupling associated with the pyridazine bridge.

The trend in $2J$ values for the diazine/azide bridged complexes, with exchange becoming progressively more antiferromagnetic with increasing azide bridge angle parallels exactly the trend observed for a series of dinuclear copper(II) complexes with comparable diazine/hydroxide combinations.[9] For the hydroxide case the increase was attributed mainly to the increasing antiferromagnetic contribution of the hydroxide with increasing bridge angle. It seems reasonable to assume that the azide bridge plays a similar role in the azide complexes. For azide bridge angles of >119° the net antiferromagnetic coupling is very strong (>460 cm^{-1}), and for compound **10** net exchange is comparable to that for the hydroxide-bridged systems with large bridge angles.

Figure 14 illustrates plots of $2J$ versus bridge angle for the azide complexes described in this study and a selection of comparable diazine/hydroxide complexes[9] (for **8**, $2J$ has been set equal to ≈−40 cm^{-1}, based on χ_{max}). Two additional data (points 14, 15) have been added for comparable diazine/μ_2-1,1-azide complexes not formally described in this study (Figure

(55) Mandal, S. K.; Thompson, L. K.; Gabe, E. J.; Lee, F. L.; Charland, J.-P. *Inorg. Chem.* **1987**, *26*, 2384.

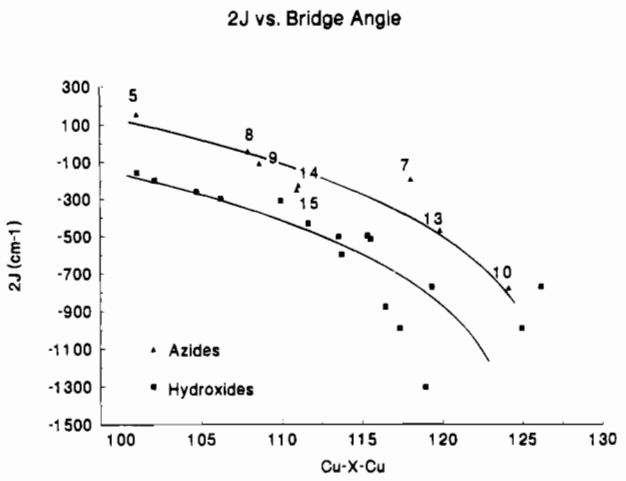

Figure 14. Plot of $2J$ (cm^{-1}) versus bridge angle for μ_2-1,1-azide- and μ_2-hydroxide-bridged dinuclear copper(II) complexes. Key: $[Cu_2(PAP6Me)(\mu_2\text{-}N_3)(\mu_2\text{-}Br)Br_2]\cdot 0.5CH_3OH$[56] (**14**); $[Cu_2(PAN)(\mu_2\text{-}N_3)(NO_3)_2](NO_3)\cdot CH_3CN\cdot CH_3OH$ (**15**) (PAN = 1,4-bis(2′-pyridylamino)naphthalazine).[56] All hydroxide data are taken from ref 9 with the following exceptions: $[Cu_2(PAP)(\mu_2\text{-}OH)(\mu_2\text{-}Cl)Cl_2]\cdot 1.5H_2O$ (Cu−OH−Cu = 101.0°, $2J = -158(1)$ cm^{-1}; remeasured); $[Cu_2(PAP)(\mu_2\text{-}OH)(\mu_2\text{-}Br)Br_2]\cdot 1.5H_2O$ (Cu−OH−Cu = 102.1°, $2J = -198(2)$ cm^{-1}; remeasured); $[Cu_2(PTP)(\mu_2\text{-}OH)(\mu_2\text{-}Cl)Cl_2]$[45] (Cu−OH−Cu = 106.2°, $2J = 297(1)$ cm^{-1}); $[Cu_2(PTPH)(\mu_2\text{-}OH)(NO_3)_2(H_2O)_2]NO_3$[41] (Cu−OH−Cu 109.0°, $2J = 308(5)$ cm^{-1}).

14, caption).[56] For both series of complexes, despite some minor spread of the points, the data appear to vary in a nonlinear fashion, with very shallow curvature for bridge angles <119 (N_3) and <116° (OH), and then a marked increase in curvature at larger bridge angles is observed (curves drawn arbitrarily). Since the curves are roughly parallel for both series, especially at lower bridge angles, it is reasonable to assume that exchange is varying in a similar way, while the dinuclear center dimensions change in a comparable fashion. This is reasonable considering the comparable nature of the bridging atoms, and trends in the Cu−N−N, diazine, angles. These fall in the ranges 113.6−116.5° (OH), 114.3−117.5° (N_3) (Chart 1b; $X = 6$), 119.3−122.3° (OH), and 122.0−122.8° (N_3) (Chart 1b; $X = 5$). For Cu−OH−Cu bridge angles in the range 100−116° the Cu−N−N angles vary only in a minor way, and so it is reasonable to interpret the magnetostructural data for the hydroxide-bridged complexes in a linear fashion, with $2J$ varying as a function of bridge angle only. In fact the data with Cu−OH−Cu <116° follow a good straight line relationship,[9] with an intercept at $2J = 0$ cm^{-1} of ≈95°, some 2.5° less than the angle for accidental orthogonality computed by Hatfield and Hodgson.[3] For the critical hydroxide bridge angle of 97.5°, $2J$ would be ≈−70 cm^{-1}, which effectively means that for a hypothetical pyridazine or phthalazine complex with this Cu−OH−Cu angle the diazine itself would propagate antiferromagnetic coupling with $2J \approx -70$ cm^{-1} (assuming $J_T = J_F + J_{AF}$ and $J_F = 0$).[3] It is of interest to note that for the complex $[Cu_2(PAP46Me)Cl_4]$, which involves just a magnetically active phthalazine bridge linking two square-pyramidal copper centers (the two additional chlorine bridges are orthogonally bound), and a Cu−N−N (diazine) bridge angle of 117.5(2)°, comparable antiferromagnetic coupling was observed ($2J = -55$ cm^{-1}).[9] On the reasonable assumption that the diazine behaves as a roughly constant, and comparable, exchange component in the azide series, simple extrapolation at $2J = -70$ cm^{-1} on the azide curve indicates that accidental orthogonality might be expected at ≈108.5°. This value is remarkable considering the fact that extended Hückel calculations predicted accidental orthogonality for the hydroxide bridge at ≈92°, and it occurs 5.5° above this value, while for the azide bridge it was calculated to be ≈103°.[2] It is of interest, and relevance, to note that for **8** net antiferromagnetic exchange is small.

The pyridazine bridge has been shown to propagate strong antiferromagnetic exchange ($2J \approx -540$ cm^{-1}), when bound as the only bridge in a flat (2:2) structure, involving a $d_{x^2-y^2}$ copper ion ground state,[53] while under similar circumstances the phthalazine bridge propagates somewhat weaker coupling ($2J \approx -490$ cm^{-1}).[51] These complexes involve equatorial Cu−N−N (diazine) bridge angles of 126.8(7), 127.3(8)° and 124.7(6), 127.5(6)°, respectively, which are somewhat larger than the 120° optimum anticipated for maximum overlap between the copper magnetic orbitals and the ligand σ framework. The azide and hydroxide bridged complexes with bridge angles >116° involve five-membered peripheral chelate rings (Chart 1b, $X = 5$). This leads to Cu−N−N angles which are somewhat larger than 120°, falling in the range 122.1−122.5° for **10** and **13** and 120.0−122.0° for the hydroxide complexes. It is reasonable to assume that as these angles approach the values for the 2:2 diazine complexes,[51,52] enhanced antiferromagnetic coupling may be expected due to the diazine bridge also. This should manifest itself as a changing slope in the graph, with increasing negative slope as the dimensions of the dinuclear center get bigger. This is evidently the case for both series of complexes (Figure 14) and clearly indicates that at large bridge angles exchange terms associated with the two bridges are comparable and strongly antiferromagnetic. To our knowledge only two previously reported examples of structurally and magnetically characterized μ_2-1,1-azide-bridged dicopper(II) complexes, which involve just equatorial azide bridges, exhibit net ferromagnetism. However, for these compounds a very narrow range of Cu−N_3−Cu angles was observed (100.5−105.46°).[15,16] The complex $[Cu_2(tmen)_2(\mu_2\text{-}N_3)(\mu_2\text{-}OH)](ClO_4)_2$, which has a 50/50 disordered bridge situation and so corresponds to an average of one hydroxide and one azide bridge, has estimated Cu−N_3−Cu and Cu−OH−Cu angles of 95.7 and 102.5°, respectively.[17] Strong ferromagnetic coupling was observed for this compound (>200 cm^{-1}), which can be rationalized assuming that the very small Cu−N_3−Cu angle would correspond to a very strong ferromagnetic term, which would more than counteract the expected antiferromagnetic term resulting from the large Cu−OH−Cu angle ($J_T = J_F + J_{AF}$).[17]

In the few cases where equatorial combinations of μ_2-1,1-azide and phenoxide bridges link the two copper(II) centers, net antiferromagnetic coupling exists,[35−37,57] and in an example involving a Cu−O(phenoxide)−Cu bridge angle of 98.4(4)° and a Cu−(μ_2-N_3)−Cu bridge angle of 104.6(5)°, in an equatorial-bridged situation involving square-pyramidal coppers, strong antiferromagnetic exchange was observed ($2J = -482$ cm^{-1}).[33] Although no correlation between Cu−O(phenoxide)−Cu bridge angle and exchange for bis(phenoxide)-bridged dicopper(II) complexes has yet been published, it has recently been demonstrated for macrocyclic dinickel(II) systems,[58] and a preliminary analysis for the macrocyclic $d_{x^2-y^2}$ copper case indicates that, for a phenoxide bridge angle of 98.4°, $2J$ should be around −660 cm^{-1}.[56] Since the observed $2J$ value is substantially less negative the azide must contribute as a ferromagnetic bridge in this case, which is consistent with our observations. In related complexes involving much larger Cu−

(56) Thompson, L. K.; Tandon, S. S.; Manuel, M. E. Unpublished results.

(57) Kahn, O.; Boillot, M.-L. In *Biological and Inorganic Copper Chemistry*; Karlin, K. D., Zubieta, J., Eds.; Adenine: Guilderland, NY, 1986; Vol. 2, pp 187−207.

(58) Nanda, K. A.; Thompson, L. K.; Bridson, J. N.; Nag. K. *J. Chem. Soc., Chem. Commun.* **1994**, 1337.

O(phenoxide)−Cu angles (107.9,[36] 106.8°[37]) net antiferromagnetism is also observed for Cu−N_3−Cu angles of 103.6 and 103.4°, respectively. Very large antiferromagnetic ($-2J \geq 1000$ cm^{-1}) terms would be expected for the phenoxide bridges in each case,[56] and so the azide must contribute as a very strong ferromagnetic bridge, for these angles, which are well within the ferromagnetic realm established by Kahn.[15-17]

While the previous cases of ferromagnetic coupling for μ_2-1,1-azide-bridged dicopper(II) complexes are consistent with the extended Hückel approach, there are clearly not enough examples, particularly with larger bridge angles, to really test the situation adequately. However, despite the absence of such examples an additional factor, the *spin polarization* effect, was proposed by Kahn to play a major role in the ferromagnetic coupling in the μ_2-1,1 case and also to account for the antiferromagnetic exchange found for the μ_2-1,3-azide-bridged cases.[1,2,7,15-17] The rationale for this approach, which involves a dominant role of the π_g molecular orbital on the azide bridge in coupling the copper(II) ions, is predicated on the fact that extended Hückel calculations for the Cu−(μ_2-1,1-N_3)$_2$−Cu case indicate that Δ, the energy difference between the b_{1g} and b_{2u} molecular orbitals for bridge angles in the range 90−110°, is small. The suggestion was made that if Δ remains small, regardless of the Cu−N−Cu angle, the antiferromagnetic contribution for larger bridge angles would be weak also and would not compensate for inherent ferromagnetism and perhaps would not account for the observed ferromagnetism for systems with azide bridge angles in the range 100.5−105.5° ($J_T = J_{AF} + J_F$; $J_{AF} = -2\Delta S$; $J_F = 2C$; S is the overlap integral and C the two-electron exchange integral).[15-17] As a result of the present study this appears not to be the case, and at large bridge angles Δ dominates leading to antiferromagnetic behavior.

Compounds **1**−**13** are composed of mixtures of bridges, and so their experimental magnetic properties should be considered to result from a combination of superexchange effects, through the various "magnetic connections" involved. For compounds **1**−**6**, which are triply bridged and involve azide bridge angles in the range 98.3−105.9°, ferromagnetic coupling dominates, while for compounds **7**−**13**, which are structurally quite different, involving just two bridge groups, the diazine and the μ_2-1,1-azide, both of which are magnetically active, antiferromagnetism dominates. Azide bridge angles for **7**−**13** fall in the range 107.9(2)−124.1(3)°, well beyond the limited range associated with the known ferromagnetically coupled dicopper/azide complexes. Clearly these complexes represent excellent examples to test the role of μ_2-1,1-azide as a magnetic bridge beyond its normal ferromagnetic realm. The net antiferromagnetic coupling observed in all these complexes is clearly azide bridge angle dependent, and the azide bridge propagates *antiferromagnetic* coupling for azide bridge angles of $> \approx 108.5°$.

Conclusion

Because of a lack of suitable examples with large (>105°) azide bridge angles, the limited magnetostructural studies carried out in the last 10 years on μ_2-1,1-azide-bridged dicopper(II) complexes have shown dominant ferromagnetism, which has fostered the idea that such behavior might prevail for any bridge angle and that *spin polarization* is the major reason for the presence of ferromagnetic coupling. The current study shows that this is not the case, and the "end on" μ_2-1,1-azide bridge behaves like any other single atom bridge, exhibiting antiferromagnetism at large bridge angles. An estimate of the critical angle for accidental orthogonality that emerges from this study (≈108.5°), is consistent with the well-established hydroxo-bridged case, and also extended Hückel theory. We are continuing our studies on other "end-on" azide-bridged complexes with the objective of further establishing the antiferromagnetic realm of this single atom bridge.

Acknowledgment. We thank the Natural Sciences and Engineering Research Council of Canada for financial support for this study.

Supplementary Material Available: Tables S1−S24, listing detailed crystallographic data, hydrogen atom positional parameters, anisotropic thermal parameters, bond lengths and angles, and least-squares planes (64 pages). Ordering information is given on any current masthead page.